GOCE DELCEV UNIVERSITY
FACULTY OF MEDICAL SCIENCES

MASTER THESIS / МАГИСТЕРСКИ ТРУД

OPTIMIZATION OF FREEZE-DRYING METHOD FOR THERAPEUTIC RITUXIMAB-1B4M KIT, RADIOPHARMACEUTICAL FOR TARGETED RADIOIMMUNOTHERAPY OF CD20+ LYMPHOMAS

ОПТИМИЗАЦИЈА НА МЕТОДАТА ЗА ЛИОФИЛИЗАЦИЈА И ДОБИВАЊЕ НА КИТ РИТУКСИМАБ-1Б4М, РАДИОФАРМАЦЕВТИК ЗА ЦЕЛНА РАДИОИМУНОТЕРАПИЈА НА ЦД20+ ЛИМФОМИ

Ментор/ Mentor: Изработил/ Made by:

Prof. Emilija Janevik   David Mwanza Wanjeh

Штип/Stip, 2017 - 2018

1

DEDICATION

This work is my special dedication to my family; my forever beloved mother especially.

ACKNOWLEDGEMENTS

ABBREVIATIONS AND ACRONYMS

NHL   Non-Hodgkin's Lymphoma

TMA   Therapeutic monoclonal antibody

ATR/FTIR   Attenuated transmittance resonance/Fourier transform infrared

RIT   Radioimmunotherapy

SEC   Size exclusion chromatography

DTPA   Diethylenetriaminepentaacetic acid

DOTA   Tetraazacyclododecane-1, 4, 7, 10-tetraacetic acid

1b4mDTPA   2-(4-isothiocyanatobenzyl)-6-methyldiethylene-triaminepen taacetic acid

HAMA   Human anti-mouse antibody

HACA   Human anti-chimeric antibody

UV-VIS   Ultraviolet – Visible spectrophotometer

TABLE OF CONTENTS

LIST OF TABLES

LIST OF FIGURES

DEFINITIONS

Conjugation The chemical attachment of a chelator molecule to an antibody.

Immunoconjugate The resultant adduct of conjugation

Cold labeling The tagging of a molecule with a non-radioactive isotope.

Chelation The complexing of a metal ion with a multi-dentate ligand.

Cake The dry product in the vial on the completion of freeze drying.

INTRODUCTION

Background

Therapeutic monoclonal antibodies (TMAs) continue to grow tremendously in their clinical importance since their first application more than thirty years ago (Ecker et al., 2015). The oncological application of monoclonal antibodies has taken the same trend since the approval of the rituximab, the first approved TMA for cancer therapy (Reichert and Valge-Archer, 2007). Anti-tumor TMAs are particularly attractive for their high specificity in antigen binding. Therefore, they offer themselves as a clinically effective tool for targeting therapy to particular tumor cell types with minimal inhibition of non-target cells. Compared to the conventional small molecule anti-tumor agents, TMAs mechanism of tumor cytotoxicity is achieved through the activation of the immune system in addition to the direct tumor cell inhibition. Indeed, the in vivo efficacy of the anti-tumor TMAs has been shown to be higher than for conventional small molecule therapeutic agents for some lymphoma types (Else et al., 2012).

However, antibody therapy is not always effective. In some patient types, tumors may be refractory or resistant to TMAs or they may relapse. A number of strategies have been devised for the improvement of TMAs for such patient types. The approaches include, among others, the synthesis of antibody-drug conjugates and therapeutic radio-antibodies; some of these have already obtained regulatory approval for clinical application (Ujjani and Cheson, 2013).

Thus, two radiolabeled TMAs have so far found approval for clinical application, ibritumomab/^{90}Y-ibritumomab tiuxetan and tositumomab/^{131}I-tositumomab for the treatment of refractory or relapsed low grade CD20+ Non-Hodgkin's Lymphomas (NHLs). The benefit of using TMAs radiolabeled with energetic particle emitting radioisotopes for the targeted tumor treatment is the additional opportunity to kill other tumors cells in the vicinity of the CD20+ tumor cells through crossfire and bystander effects. The ability to kill non-CD20+ tumor cells is highly beneficial, especially where the tumor exhibits heterogeneity in antigen expression. The tissue range of the emitted particles, their therapeutic efficacy and also normal tissue toxicity depend on the energy of the particles, which in turn is dictated by the particular radioisotope used.

A variety of suitable particle emitting radioisotopes is available for radiolabeling TMAs for the radioimmunotherapy (RIT) of tumors. These radioisotopes differ in terms of

their decay modes, half-lives, particle energies and chemistry. In the RIT of CD20+ NHL, products that have seen approval for clinical application have been radiolabeled with the beta-emitters; Yttrium-90 (ibritumomab/^{90}Y-ibritumomab tiuxetan) ("Approval Letter - Ibritumomab Tiuxetan, (Zevalin), IDEC Pharmaceuticals Corp - ucm113489.pdf," n.d.) and Iodine-131 (tositumomab/^{131}I-tositumomab) ("Therapeutic Biologic Applications (BLA) > Bexxar Approval Letter 6/27/03," n.d.). Other clinically useful radioisotopes include Lutetium-177, Re-188, Samarium-153, etc. Generally, radioisotopes emitting long tissue range beta particles may be more useful for large tumor masses, while low tissue range beta particle emitters may be more useful for small tumor masses, including small metastatic lesions.

Radiolabeling of the TMAs can be achieved either directly or indirectly (Sugar et al., 2014). The direct approach is feasible for radioiodination but it is unsuitable for most radiometal labeling work because TMAs lack strong chelating groups to strongly bind the radiometal cations. For clinical usefulness of a TMA based radiopharmaceutical, the in vivo thermodynamic and kinetic stability of the metal complex is vital. Hence, derivatization of the TMAs to introduce strong chelator groups is necessary. Chelator groups that are potentially useful for a variety of radiometals have already been synthesized and widely studied (Brechbiel, 2008). For trivalent radiometal cations such as lutetium or yttrium, the commonest are DOTA derivatives and DTPA derivatives. As an already available clinical example, derivatization of ibritumomab was done with tiuxetan for radiolabeling with yttrium-90 (Jacobs, 2007).

All the currently approved RIT radiopharmaceuticals are formulated as liquid preparations. The challenges associated with such formulations are stability of the antibody in storage and a cumbersome radiolabeling process. The stability of antibodies in their low concentration solutions is low, hence their short shelf life and strict cold-chain transportation and storage. The cumbersome radiolabeling procedure increases the risk of mix-ups and poor quality of the injected preparation. For that reason, it is necessary to produce a more stable preparation that is easier to radiolabel, preferably in a one-step process; it has a long shelf life in storage and does not require strict cold-chain conditions during distribution. One strategy is to use the freeze drying technology.

Freeze drying is a widely applied, widely studied technology. It helps to produce dry

preparations of thermolabile drug substances with high porosity and fast dissolution during reconstitution. Its application in the production of biotechnological pharmaceutical products is already well established (Ekenlebie et al., 2016). The freeze drying process removes almost all the water from the solution, thereby yielding a more stable product that weighs less, and is easy and fast to reconstitute.

In our work, we intended to investigate the suitability of our freeze drying protocol for the preparation of a ready-to-use radiolabel freeze dried rituximab-1b4mDTPA kit   radiopharmaceutical for radiolabeling with yttrium-90 or lutetium-177.

LITERATURE REVIEW

Non-Hodgkin's lymphomas - NHL

Lymphomas are a heterogeneous array of malignant tumors of the lymphoid system. They are broadly grouped into Hodgkin's and Non-Hodgkin's lymphomas. The NHLs are estimated to be the sixth most frequently diagnosed tumor types. Their incidence of 85% of the incidence of all lymphomas is much higher than that of HL (Siegel et al., 2017).

The NHLs are also a heterogeneous group of about 60 tumor types that can either be indolent or aggressive, the indolent being the commonest (Siegel et al., 2017).

B cell lymphomas are more common than T cell lymphomas, accounting for about 80% of all lymphomas. Specific tumor cell antigens distinguish between B-cell lymphomas and T cell lymphomas. Cell surface antigens that are specific for B-cells and commonly used clinically include CD20, CD79a and CD19 (Adams et al., 2009).

CD20 is the most clinically important tumor marker for B cell lymphomas for the reason that, in addition to its being encountered in over 90% of all B cell NHLs (Delgado et al., 2003), it has also been successfully targeted for therapy of B cell lymphomas in over a million patients in about two decades (Boross and Leusen, 2012). CD20 is a 35kDa B cell specific transmembrane glycosylated phosphoprotein. Its function is not known for certain, but it has been shown to act as a calcium ion channel. It has also been shown to participate in the regulation of B cell cycle progression and proliferation.

It is expressed by both tumor B cells and normal B cells. In normal B cells, CD20 expression is dependent on the developmental stage of the B cells, starting from the pre-B cell all the way to mature B cells, but it is uncommon in plasma cells (Uchida et al., 2004).

Treatment options and treatment responses of NHLs vary depending on the tumor type. Since almost all B cell NHLs are CD20+ (Delgado et al., 2003), antiCD20 TMAs are particularly useful. AntiCD20 TMA based medications that have been approved for therapy of lymphomas include rituximab, obinutuzumab, ibritumomab - [90]Y and tositumomab – [131]I.

Rituximab

Rituximab is a type I anti-CD20 chimeric IgG 1 kappa TMA, bearing human derived constant regions and mouse derived variable regions. It has a molecular weight of 143859.7Da and the molecular formula of $C_{6416}H_{9874}N_{1688}O_{1987}S_{44}$.

It is composed of two light chains of 213 amino acids each and two heavy chains with 451 amino acids each as follows (DrugBank, 2016):

Rituximab heavy chain chimeric

QVQLQQPGAELVKPGASVKMSCKASGYTFTSYNMHWVKGLEWIGAIYPGNGDTSYNQKFKGKATLT
ADKSSSTAYMQLSSLTSEDSAVYYCARSTYYGGDWYFNVWGAGTTVTVSAASTKGPSVFPLAPSSK
STSGGTAALGCLVKDYFPEPVTVSWNSGALTSGVHTFPAVLQSGLYSLSSVVTVPSSSLGTQTYICN
VNHKPSNTKVDKKAEPKSCDKTHTCPPCPAPELLGGPSVFLFPPKPKDTLMISRTPEVTCVVSHEDP
EVKFNWYVDGVEVHNAKTKPREEQYNSTYRVVSVLTVLHQDWLNGKEYKCKVSNKALPAPIETISKA
KGQPREPQVYTLPPSRDELTKNQVSLTCLVKGFYPSDIAVEWESNGQPENNYKTTPPVLDSDGSFFL
YSKLTVDKSRWQQGVSCSVMHEALHNHYTQKSLSLSPGK

Rituximab light chain chimeric

QIVLSQSPAILSASPGEKVTMTCRASSSVSYIHWFQQKPGSSPKPWIYATSNLASG
VPVRFSGSGSGTSYSLTISRVEAEDAATYYCQQWTSNPPTFGGGTKLEIKRTVAAP
SVFIFPPSDEQLKSGTASVVCLLNNFYPREAKVQWKVDNALQSGNSQESVTEQDS
KDSTYSLSSTLTLSKADYEKHKVYACEVTHQGLSSPVTKSFNRGEC
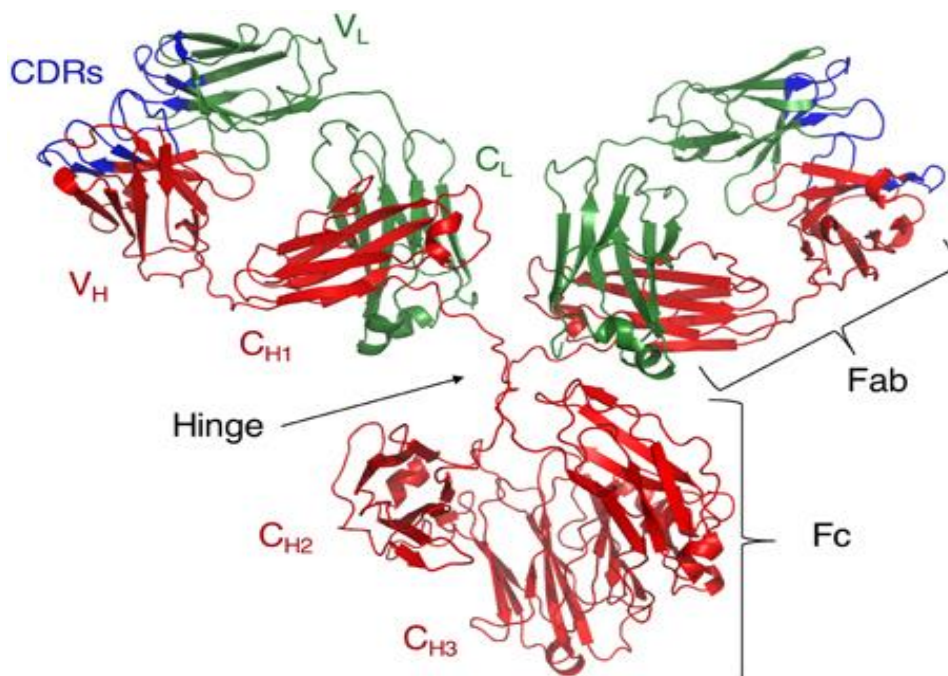
Fig 1. Graphical representation of the structure of a monoclonal IgG antibody (Janda et al., 2016).
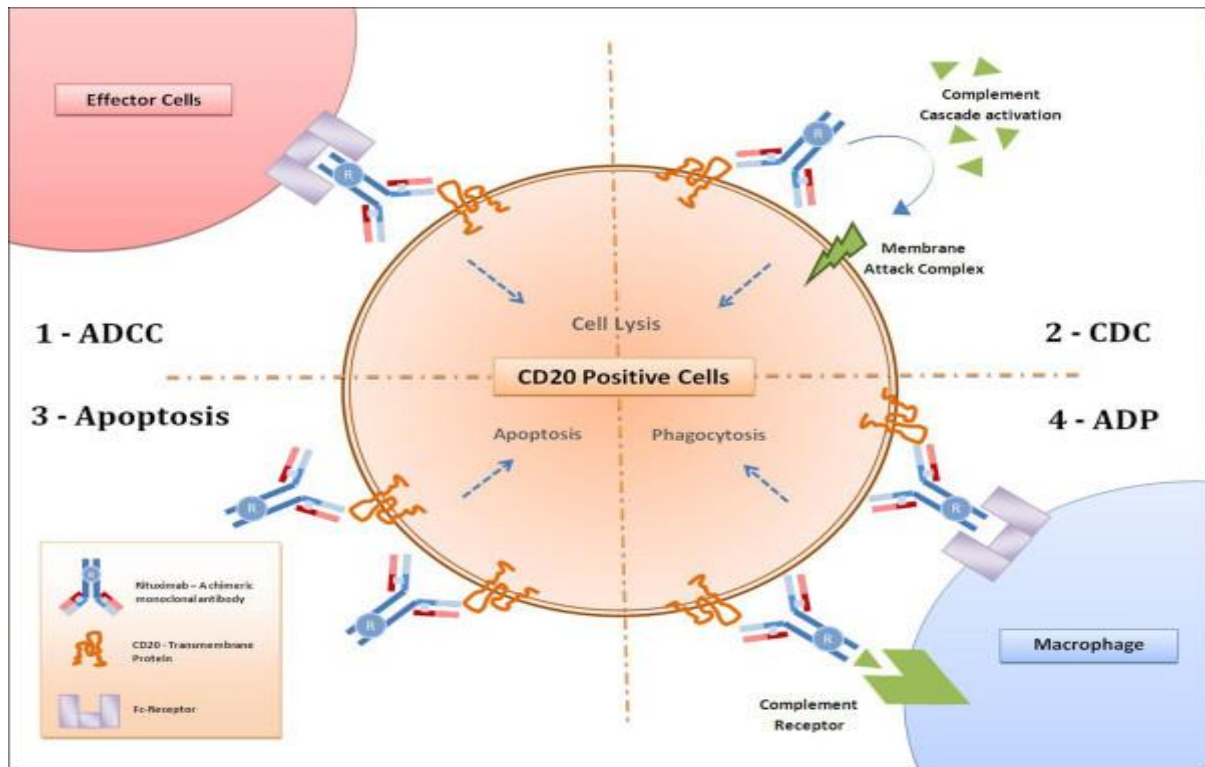
Figure 2. Proposed mechanism of action of rituximab. (Kasi et al., 2012)

Rituximab is able to exert in vivo biological effects through a number of processes which are mainly antibody-dependent cell-mediated cytotoxicity (ADCC), complement-dependent cytotoxicity (CDC) and direct induction of apoptosis (Boross and Leusen, 2012). For its ADCC effect, the TMA binds to its specific CD20 antigen on the cell surface of the B tumor cell through its complementarity determining regions (CDR) within the variable regions, while its Fcγ region binds to and activates cytolytic immune cells such as natural killer (NK) cells, T cells, macrophages, etc. For the CDC process, which is a feature of type I antiCD20 TMAs, the antibody binding to the antigen causes the reorganization of lipid rafts on the cell membrane that activate complement, development of membrane attack complex and cell lysis. Meanwhile, apoptosis results from the activation of the apoptosis pathways as an effect of the direct binding of the TMA to the CD20 antigen.

Rituximab, the first FDA approved antiCD20 TMA, is applied today for the treatment

of B cell lymphomas alone or in combination with chemotherapy, radiotherapy or radi-oimmunotherapeutic agents. Rituximab-based regimens are very effective for CD20+ lymphomas and cure rates of 50% are usually achieved for patients with some forms of aggressive NHLs (Johnston et al., 2010). For indolent types, responses to therapy are lower. Despite CD20 expression, some patients are either refractory or they relapse following rituximab based regimens. Resistance to rituximab is currently estimated to range from 30% to 60%, only less than a third of which have been found to have lost CD20 expression post rituximab therapy (Rezvani and Maloney, 2011). Such findings have necessitated the development of approaches geared towards improving therapeutic outcomes, including the development of new antiCD20 TMAs and radio-immunotherapeutics. Radioimmunotherapeutics that have already been approved for lymphomas, especially indolent refractory or relapsed NHLs, are ibritumomab-^{90}Y and tositumomab-[131]I. In clinical trials, radioimmunotherapeutics showed much better efficacy and tolerability than immunotherapy alone (Witzig et al., 2002).

Therapeutic radionuclides (Yttrium-90 and Lutetium-177)

Since the first report of the beneficial effects of injected radio-radium in 1913, the array and application of particle emitting radioisotopes in clinical practice has grown tremendously (Yeong et al., 2014).

They are a group of diverse radionuclides with differing chemical and physical properties. Nonetheless, the common feature of therapeutic radionuclides is that they are particle emitters with a high linear energy transfer (LET).

Currently, the most commonly used radionuclides are beta and alpha particle emitters. Examples of beta particle emitters are iodine-131, yttrium-90, and lutetium-90 while examples of alpha emitters are radium-223 and astatine-211.

Table 1 below summarizes the most commonly encountered therapeutic radionuclides (Yeong et al., 2014).

Table 1. Features of common clinically used therapeutic radionuclides (Yeong et al., 2014), (Srivastava and Mausner, 2013)

Radionuclide	Mode of decay	Half-life	E-max (MeV)	Maximum soft tissue range (mm)	Imageable	Gamma energy (keV)
^{90}Y	β−	2.7d	2.3	11	No	-
^{177}Lu	β−	6.7d	0.5	1.7	Yes	208
^{131}I	β−, γ	8.0d	0.6	2.4	Yes	364.5
^{89}Sr	β−	50.5d	1.5	8.0	No	-
^{188}Re	β−, γ	17h	2.1	11	Yes	155
^{186}Re	β−, γ	3.7d	1.1	3.2	Yes	137
^{153}Sm	β−, γ	46.5h	0.8	3.1	Yes	103
^{32}P	β−	14.3d	1.7	7.9	No	-

The choice of the radionuclide to be used in the development of radiopharmaceuticals depends on the radionuclide's availability and also on its physical properties, chemical properties and biological properties, all of which should be matched with the intended clinical use of the radiopharmaceutical. Physically, the   radionuclide should have a high yield of particle radiations of appropriate energy. The half-life, especially for anti-body-based radiopharmaceuticals, should be matched appropriately with the in vivo pharmacokinetics of the targeting antibody. Since the biological half-life of many TMAs is about three days, it is desirable that therapeutic radionuclides for radiolabeling TMAs should have physical half-lives of about three to seven days. Shorter lived ones may not allow for sufficient accumulation of radioactivity at the tumor site, while a too long half-life may expose patients to   excessive radiation doses apart from their lower efficacy. Ideally, therapeutic   radionuclides should be devoid of non-particulate radiation. However, the concurrent emission of suitable energy gamma

rays is in fact a desired feature of 'ideal' theranostic radionuclides since it facilitates dosimetry and monitoring of the therapy. The emitted particles must also be of suitable energy. If the energy is too high, toxicity to non-target tissues is likely to be higher than acceptable, whereas low energy particles are likely to be ineffective. Alpha particles are of high energy, but since their tissue range is very low, their LET is very high and suitable for treating tumor micro-metastases. On the other hand, beta particles have variable energies and the high energy betas are more penetrating but with low LET. For that reason, radioisotopes that emit high energy betas are suitable for targeting large tumor masses. Since lower energy betas have very high LET and low tissue range, they are more suitable for targeting tumor micro-metastases than large tumor masses. In addition to the above is the requirement for a suitable chemistry of the radionuclide. The chemical properties of the radioisotope should permit a fast, strong and kinetically stable attachment of the radionuclide to the targeting molecule. Of equal importance is the availability of the radioisotope. A radioisotope that is too diffi-cult to obtain in adequate amounts is unlikely to be of any appreciable benefit to patient care.

Yttrium is a group III element with atomic number 39 and electronic configuration of [Kr] $4d^1$ $5s^2$. The clinically important therapeutic radioisotope is Yttrium-90. Yttrium-90 decays 100% by emitting beta particles to zirconium-90 in a half-life of 2.67 days (MM Be, 2004). Its beta particles have a maximum energy of about 2.3 MeV and their maximum tissue penetration is 11mm, as shown in Table 1 above. The chemistry of yttrium is similar to that of the lanthanides, which is dominated by its +3 oxidation state. It forms complexes that are highly stable, both thermodynamically and kinetically, with multi-dentate ligands containing hard donor ligands such as amine groups and car-boxylate groups. Examples of the chelators are shown in Table 2 below. Yttrium-90 is commercially available mostly from strontium-90/yttrium-90 generators and also from neutron irradiation of yttrium-89 (Be MM, 2004).

The production and purification of the radionuclide is done at the radionuclide suppli-ers' premises and availed to the compounding radiopharmacies as $^{90}YCl_3$. Yttrium-90 is already used today in ibritumomab-tiuxetan-^{90}Y for the therapy of indolent refractory or relapsed NHL and also for radioembolization with microspheres for ther-apy of hepatocellular tumors (Davies, 2007) (Bhangoo et al., 2015).

Lutetium is a lanthanide element, with atomic number 71 and electronic configuration of [Xe] $4f^{14}5d^{1}6s^{2}$. Lutetium-177 is the commonest applied lutetium radioisotope for internal dose radiotherapy. It decays 100% through beta emission to hafnium-177, in a half-life of 6.65 days (MM Be 2004 Vol. 2-A= 151 to 242). The beta particles of lutetium-177 have maximum energy of 497.8 keV and a maximum tissue range of 1.7 mm, as shown in Table 1 above. Like other lanthanides, the chemistry of lutetium is dominated by its +3 oxidation state. Its stable complexes are those with multi-dentate ligands composed of hard donor ligands such as amine groups and carboxylate groups, in which its coordination numbers range from 6 to 9 (L. Parus et al., 2015). Examples of chelators that are useful in the radiopharmaceutical chemistry of lutetium are given in Table 2 below. Lutetium-177 is produced in nuclear reactors by neutron irradiation of lutetium-176 or from the neutron irradiation of ytterbium176 followed by beta decay of the resultant ytterbium-177 MM Be 2004 Vol. 2-A= 151 to 242). It is supplied to radiopharmacies as $^{177}LuCl_3$. Lutetium-177 is currently applied in ^{177}Lu-DOTATATE for therapy of somatostatin receptor (SSTR) overexpressing neuroendocrine tumors (NET) (Strosberg et al., 2017).

Radiolabeling of antibodies

The radiolabeling of antibodies can be achieved either directly or indirectly depending on the chemistry of the radioisotopes (Tolmachev et al., 2014). The direct radiolabeling approach is suitable for radionuclides whose chemistry allows them to be bonded directly and strongly to the amino acid residues on the antibody molecules.
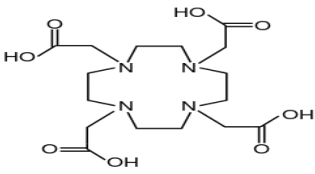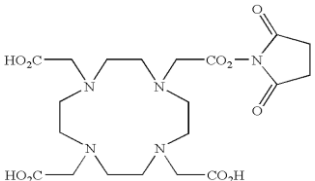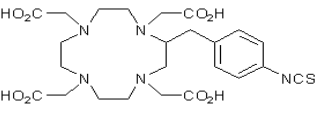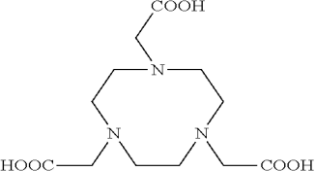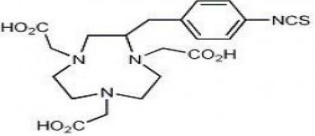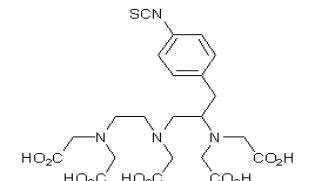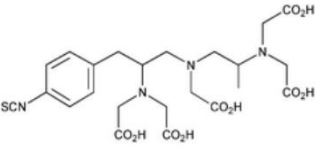
Radiohalogenation is a classic example of this. Direct radioiodination has been employed successfully for the production of therapeutic radioimmunopharmaceuticals such as tositumomab-[131]I. Attractive as it is, direct radiolabeling of antibodies is not always feasible, especially for labeling with most radiometals. Usually, antibodies lack the suitable arrangement of donor groups for strong chelation with radiometals. For that reason, the indirect radiolabeling method is used, which requires derivatization of the antibodies with suitable bifunctional chelator (BFC) molecules either before or during the radiolabeling process. There are two ways the indirect approach can be effected; one is the pre-labeling method and the other is the post-labeling method (Liu, 2008). In the pre-labeling method, the radiometal is chelated with the BFC and the

resultant chelate is conjugated to the antibody via reactive groups on the amino acid residues. The advantage of this method is that it is less aggressive on the antibody structure since it avoids exposing the antibody to the harsh conditions of chelation chemistry. However, it is difficult to implement radiopharmaceutical kit formulation with this method. Therefore, the post-labeling method became more attractive and more popular due to the desire to produce ready-to-label kit radiopharmaceuticals. In this post-labeling method, the antibody is first conjugated with the BFC, purified and then mixed with the radiometal to effect the radiolabeling. This method is currently used for the production of ibritumomab-^{90}Y, which is supplied as a liquid kit radiopharmaceutical where ibritumomab is already conjugated with tiuxetan, ready to radiolabel by mixing with ^{90}YCl$_3$ solution ("Zevalin_Package_Insert.pdf," n.d.).

In view of the foregoing, the growing importance of BFCs in radiopharmaceutical production cannot be overemphasized. Depending on the functional groups on BFC, the conjugation amino acid residues on the antibody molecules will vary. The commonest employed BFCs are designed to attach covalently through amide or thioamide bond formation with the epsilon primary amino groups of lysine residues (Sugiura et al., 2014). Since the charge of the free amine groups may be vital for the antibody function, the conjugation at these groups needs to be carefully crafted. Also, a large number of BFC groups may alter the antibodies' CDRs steric fitting onto the antigen binding sites. On the other hand, fewer than optimal BFCs may decrease the specific activity of the radiopharmaceutical with consequent decrease in therapeutic efficacy. In addition to the above concerns, the chemically altered antibody may have significantly different in vivo pharmacokinetics from the parent antibody. It is therefore necessary to evaluate the TMA based radiopharmaceutical from physicochemical properties, in vitro antigen binding studies to in vivo studies because the assumption that the radiopharmaceuticals' pharmacokinetics would be similar to those of the   parent antibody is not always accurate.

Below is a list of the commonly encountered BFCs for radiolabeling in yttrium and lutetium based radiopharmaceuticals (Brechbiel, 2008).

Table 2. Commonly used bifunctional chelating agents (L. Parus et al., 2015)

Structure	Name	Acyclic/cyclic
	DOTA	Cyclic
	DOTA-NHS ester	Cyclic
	p-SCN-Bn-DOTA	Cyclic
	NOTA	Cyclic
	p-SCN-Bn-NOTA	Cyclic
	p-SCN-Bn-1B-DTPA	Acyclic
	p-SCN-Bn-1B4M-DTPA	Acyclic

Freeze drying

Freeze drying is the process of removing water from a product mainly through sublimation. The technology is very useful for the drying of thermolabile drug substances, for example protein-based and biotechnological products. Water can promote the hydrolysis of biotechnological and protein based drug substances, especially dilute solutions, thereby shortening the products shelf life. In their dry state, however, these drug products are less bulky, more stable and they can be transported and stored at higher temperatures. Their shelf lives can also be extended significantly. The cycle of freeze drying follows three main steps: freezing, primary drying and secondary drying. The quality of a freeze dried product depends heavily on the efficiency of the freeze drying process.

In the freezing step, the aqueous product is cooled to temperatures and for durations that ensure a complete conversion of the product to solid. As the temperatures are lowered, it reaches a point where ice nucleation starts randomly within the solution. As the ice crystals grow with further cooling, the water separates (as ice) from the unfrozen product, which becomes increasingly saturated and is called a freeze concentrate. On further cooling, the freeze concentrate turns viscous and later glassy at the glass transition temperature. Freezing is conducted at much lower temperatures than the glass transition temperature. The freezing is required to occur uniformly throughout the formulation so as to yield a dry product with uniform pore size and other parameters. An annealing step can be introduced so as to facilitate uniform freezing. Annealing step involves elevating the temperature of the frozen sample, holding it at the annealing temperature and then lowering it back to the freezing temperature to continue with the freezing step. Annealing has been shown to facilitate faster, complete uniform freezing (Abdelwahed et al., 2006) (Chouvenc et al., 2006). The annealing temperature is usually below or at the glass transition temperature of the formulation. The temperature at which the viscous matrix turns back to free-flowing liquid on reheating is the melt or collapse temperature. The temperatures are unique for different formulations. For efficient freeze drying, it is important for these temperatures to be known for the particular formulations being freeze dried. Knowledge of these temperatures informs the decision on the primary drying temperature because even though primary drying has been successfully performed at or slightly above the glass

transition temperature, it should not be performed at or above the collapse temperature. The freezing rate has major implications on the product characteristics (Lee and Cheng, 2006), such as pore size, final moisture content etc, and also to the required drying time.

The primary drying step requires input of heat energy into the product so as to facilitate sublimation. It is usually the longest phase of the freeze drying process. The sublimation of the ice causes increased water vapor partial pressure within the drying chamber. For the drying step to proceed efficiently, the liberated water vapor must be extracted from the drying chamber since the driving force for the drying process is the water vapor partial pressure gradient between the drying chamber and the immediate environment. As the product becomes drier, so increases the collapse temperature such that secondary step drying can be done at even higher temperatures.

At the end of primary drying, residual sorbed (bound) moisture of about 5-10% w/w remains (Patel et al., 2010). During the secondary drying step, the bound moisture is removed by desorption. If primary drying is done well enough, the secondary drying can be performed at room temperature depending on the collapse temperature of the formulation. The desired final moisture content after secondary drying varies from one drug substance to another. Proteinaceous substances generally require higher final moisture content than small molecular substances. Too high moisture content yields a poor stability product while too low moisture content causes structural, and hence functional, damage to the protein-based substances. Excessively dehydrated protein-based substances tend to have higher opalescence and longer reconstitution times on reconstitution. Generally, protein-based substances can be dried to moisture content of 1% – 3% w/w (Schneid et al., 2011).

For a successful freeze drying, critical formulation characteristics and critical process parameters must be identified and controlled. One critical formulation characteristic is the collapse temperature. The desire is to have a formulation with as high a collapse temperature as possible. Freeze drying is an expensive process in terms of electrical power consumption. A higher collapse temperature allows for the freezing and primary drying phases to be done not only at higher temperatures, but also for shorter times and more effectively. Since the freeze drying process is highly stressful to the drug substances, especially proteins, it is desirable also that the process takes

as short a time as possible. One method to influence the collapse temperature of a formulation is to incorporate carefully selected excipients.

Excipients can have a profound effect on the freeze drying process. Excipients used in freeze drying include buffers, tonicity modifiers, bulking agents, surfactants, cryoprotectants, lyoprotectants, modifiers of collapse temperature, antioxidants, etc. For radiopharmaceutical products, however, the target is to incorporate as few as necessary excipients. The choice of the excipients relies on their necessity and their compatibility with the radioisotope label. Especially for kit radiopharmaceuticals for radiolabeling with radiometals, it is vital to ensure that none of the excipients binds the radioisotope.

MATERIALS AND METHODS

Materials

1. Orbital shaker, MRC

2. Falcon 15ml conical centrifuge tubes

3. Ultracel® - 30K, Millipore, Ireland

4. Labconco Free Zone Stoppering Tray Dryer, (USA)

5. Oakton Acorn pH 6 Meter

6. Medical Fridge, Liebherr LKv 3913

7. Laminar flow cabinet, Miniflo Due type 120

8. Jenway UV/VIS spectrophotometer 6715

9. Phosphate buffer 0.1M, pH 8.0

10. Rituximab 500mg/50ml, Mabthera®, Roche Co, CA, USA,

11. Ammonium Acetate 50mM buffer pH 5.5

12. Gel filtration 10mL Sephadex-25G columns

13. Yttrium chloride powder, Sigma

14. Lutetium chloride powder, Sigma

15. 1b4m-DTPA powder, Sigma

16. FTIR Spectrometer, PARAGON 1000, Perkin Elmer

17. Raman Spectrometer, Horiba JobinYvon LabRam 300 Infinity, with Olympus MPlanN confocal microscope.

Methods

Purification of rituximab from MabThera®

2ml of the commercial product (MabThera®) was loaded into Amicon 2ml 30kDa ultrafilters and ultrafiltered at 5000 rpm in 4 cycles of one hour per cycle at 2-8°C. 2ml of 0.1M phosphate buffer pH 8.0 was added to the ultrafilter at the end of every cycle. The ultrafiltrate was discarded. After the 4th cycle, the purified rituximab was recovered by reverse filtration at 5000rpm for one hour. The product was reconstituted to 2ml with 0.1M pH 8.0 phosphate buffer and stored at 2-8°C temperatures in 15ml falcon conical centrifuge tubes.

Freeze drying of rituximab

Samples of rituximab formulations were freeze dried, some using the already established three day protocol and others using the new two-day protocol.

For the three-day protocol, 1ml aliquots of purified 1mg/ml rituximab in 0.1M phosphate buffer pH 8.0 were dispensed into 10ml type 1 glass vials at 2-8°C. The vials were partially closed with the lyophilization metal-free rubber stoppers and loaded into the freeze drier at shelf temperature of 4°C. The shelf temperature was then lowered at a rate of 0.4°C/min to -40°C. It was held at -40°C for 3 hours and an annealing step was added for the freezing phase to complete in 10 hours before the vacuum pump was turned on. During the annealing, the shelf temperature was raised at a rate of 0.2°C/min to -15°C, held for 5h and then lowered back to -40°C at the same rate. The subsequent phases were performed at chamber pressures of 0.12mBar. At a rate of 0.2°C/min, the shelf temperature was raised to -10°C and held at the -10°C for 25 hours for the primary drying phase. At the end of the primary drying phase, the shelf temperature was elevated at a rate of 0.4°C/min to 25°C and held at the 25°C for 11 hours for the secondary drying phase. After the secondary drying phase, the chamber vacuum was released with atmospheric air. The vials were then automatically stoppered and stored at 2-8°C pending further investigations.

For the two day protocol, 1ml aliquots of purified 1mg/ml rituximab in 0.1M phosphate buffer pH 8.0 were dispensed into 10ml type 1 glass vials at 2-8°C. The vials were partially closed with the lyophilization metal-free rubber stoppers and loaded into the freeze drier at a shelf temperature of 4°C. The shelf temperature was then maintained

at 4°C for 30min. Then, it was lowered at a rate of 1°C/min to -40°C, held for 5 hours for the freezing phase before the vacuum pump was turned on. The subsequent phases were performed at chamber pressures of 0.12mBar. At a rate of 0.15°C/min, the shelf temperature was raised to -10°C and held at the -10°C for 15 hours for the primary drying phase.

At the end of the primary drying phase, the shelf temperature was elevated at a rate of 0.2°C/min to 25°C and held at the 25°C for 11 hours for the secondary drying phase. At the end of secondary drying, the chamber vacuum was released with atmospheric air. The vials were stoppered and stored at 2-8°C pending further investigations.

Conjugation

2ml of the rituximab purified product was pipetted into a 15ml Falcon centrifugation tube, into which 1.54mg in 0.154ml of 1b4mDTPA in 0.1M phosphate buffer pH 8.0 was added to make a rituximab-to-1b4mDTPA mole ratio of 1:20. The mixture was then mounted on an orbital shaker in 2-8°C and left to react overnight (for 18 hours) at shaker speed of 50rpm.

Purification of immunoconjugate

The reaction mixture was loaded onto 2ml Amicon 30kDa ultrafilters and ultra-filtered at 5000 rpm in 2-8°C for 4 one-hour cycles, washing with 2ml of 0.1M pH 8.0 phosphate buffer in each cycle. After every cycle, the absorbance of ultrafiltrate at 280nm wavelength in a uv-vis spectrophotometer was determined and the ultrafiltration continued until the ultrafiltrate absorbance was zero (after the 4th cycle).

The purified immunoconjugate was recovered from the ultrafilters by reversing the ultrafilters and centrifuging at 500rpm for one hour.

Concentration determination by UV-VIS spectrophotometry

The purified immunoconjugate was reconstituted to 1ml using 0.1M phosphate buffer pH 8.0. An aliquot of 0.100ml was drawn therefrom, reconstituted to 1ml with 0.1M phosphate buffer pH 8.0 and its concentration determined using UV-VIS spectrophotometry at 280nm wavelength.

Freeze drying of the immunoconjugate

Freeze drying of the immunoconjugate was performed using the two-day freeze drying

protocol as described under freeze drying of rituximab above.

'Cold' labeling and purification of 'cold-labeled product

Two vials were used for chelating, one vial for chelation with stable Lutetium and the other for chelation with stable Yttrium. One of the vials was reconstituted with 1ml 0.05M acetate buffer pH 7.0 for chelation with stable Lutetium. The other vial was reconstituted with 1ml 0.05M acetate buffer pH 5.5 for chelation with stable Yttrium.

A 10 mL solution of LuCl3 1.0709mg/ml in 0.05M HCl (Solution A) was prepared. A 100mcl solution of YCl3 11.555mg/ml (that is 5.7775mg in 50mcl) in 0.05M HCl (Solution B) was also prepared. A 10ml solution of EDTA 0.01M in metal-free distilled water was prepared and its pH adjusted to 6.0 (Solution C).

10mcl of solution A was added and into one of the vial containing 1mg rituximab-1b4mDTPA immuno-conjugate reconstituted with 0.05M acetate buffer pH 5.5. The reaction mixture was incubated at room temperature for 30min (Mixture I). , 61mcl of Solution C was added into Mixture I and incubated for 15min at room temperature. Then, the mixture was purified by washing through a 10ml G25 Sephadex column with phosphate buffer pH 8.0 into 1ml fractions. High concentration fractions (fractions 4 and 5) were collected and the rest was discarded. The purified product was stored in type I glass vials in refrigerator pending further manipulation.

Into the other vial containing 1mg of rituximab-1b4mDTPA immuno-conjugate reconstituted with 0.05M acetate buffer pH 5.5, 30mcl of Solution B was added and mixed. The reaction mixture was incubated at room temperature for 30min (Mixture II).

Then 63mcl of Solution D was added into Mixture II, mixed and incubated at room temperature for 15min. Then, the mixture was purified by washing through a 10ml G25 Sephadex column with phosphate buffer pH 8.0 into 1ml fractions. High concentration fractions (fractions 4 and 5) were collected and the rest was discarded. The purified product was stored in type I glass vials in refrigerator pending further manipulation.

Analysis

1. **Fourier Transform Infrared (FTIR) spectroscopy**

For this investigation, both solid and liquid samples were investigated. Firstly,

investigations were made on the rituximab commercial product (MabThera®), purified non-freeze dried rituximab, non-freeze dried immunoconjugate of 1b4mDTPA, yttrium chelated non-freeze dried immunoconjugate and lutetium chelated non-freeze dried immunoconjugate. Secondly, investigations were made on the freeze dried rituximab, freeze dried immunoconjugate, yttrium chelated freeze dried immunoconjugate and lutetium chelated freeze dried immunoconjugate.

Liquid samples

The investigated liquid samples were of rituximab commercial product, purified rituximab, freeze dried rituximab from 3-day freeze drying protocol, freeze dried rituximab from 2-day freeze drying protocol, non-freeze dried immunoconjugate, 2-day freeze dried immunoconjugate, yttrium chelated freeze dried immunoconjugate, yttrium chelated non-freeze dried immunoconjugate, lutetium chelated freeze dried immunoconjugate and lutetium chelated non-freeze dried immunoconjugate. The freeze dried rituximab and freeze dried immunoconjugate were reconstituted with 1ml 0.9% saline solution for the investigation while the purified rituximab, non-freeze dried immunoconjugate, yttrium chelated immunoconjugates and lutetium chelated immunoconjugates were investigated as solutions in 0.1M phosphate buffer pH 8.0.

A background scan was taken on an empty crystal surface. Then, a drop from the products was drawn with spatula and applied onto the mounting plate so as to cover the crystal surface of the ATR-FTIR spectrometer and scanned with wavenumber range of 4000 – 800 cm^{-1}. The mounting plate was cleaned with an alcohol swab prior to scanning of subsequent samples.

Solid samples

The investigated solid samples were of freeze dried rituximab via the 3-day protocol, freeze dried rituximab via the 2-day protocol and freeze dried immunoconjugate.

A background scan was run on an empty crystal surface. Then, a small but enough amount of the solid powder was applied onto the mounting plate as to cover the crystal surface. The pressure knob was placed on top of the sample and screwed until it double-clicked into position. Scanning was done at wavenumber range of 4000 – 800 cm^{-1}. The mounting plate was cleaned with alcohol swab.

RESULTS

Purification of rituximab from commercial product MabThera®

Rituximab used in my work was obtained from the commercial product MabThera®. Because this commercial product was dedicated for application in patients   it contained some additives and stabilizer. For the realization of our experiments we needed the pure antibody. For that reason, we purified the commercial product using ultrafiltration.

During the process of ultrafiltration as it is described in methods, we wanted to eliminate all other substances and fragments of the antibody obtained during the process of ultrafiltration.

We used Size exclusion chromatography (SEC) to confirm the purity and presence of the whole rituximab as shown in Fig. 3 and 4 below.
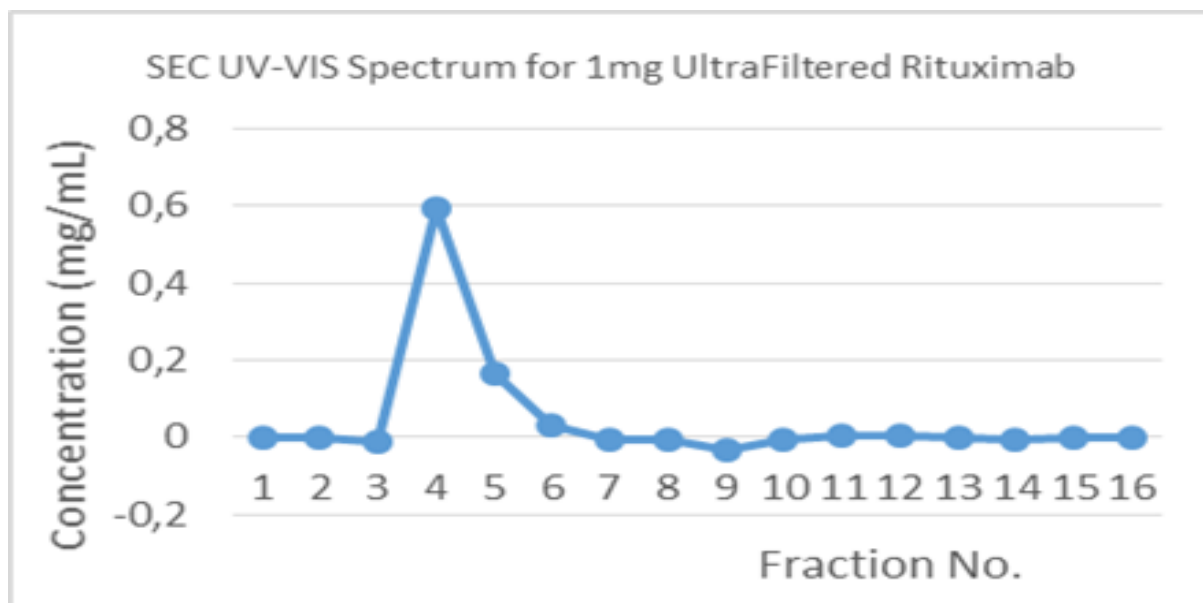

Figure 3. Size exclusion chromatography with UV-VIS detection for purified rituximab
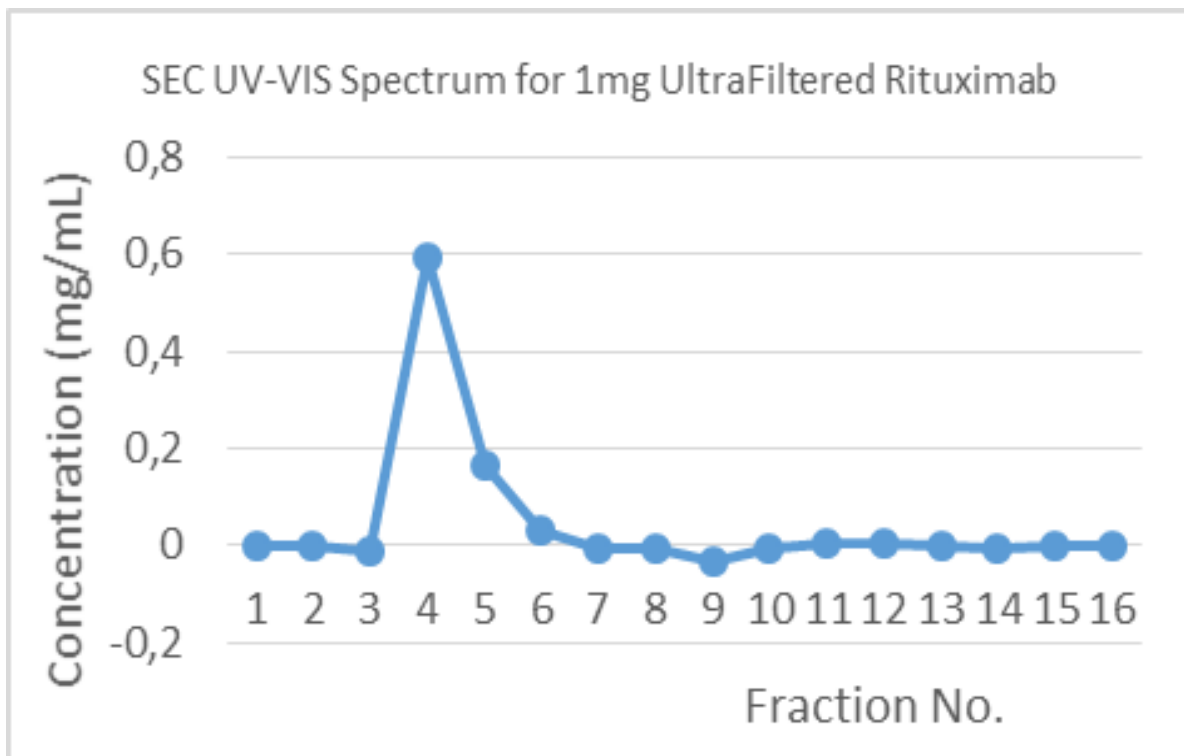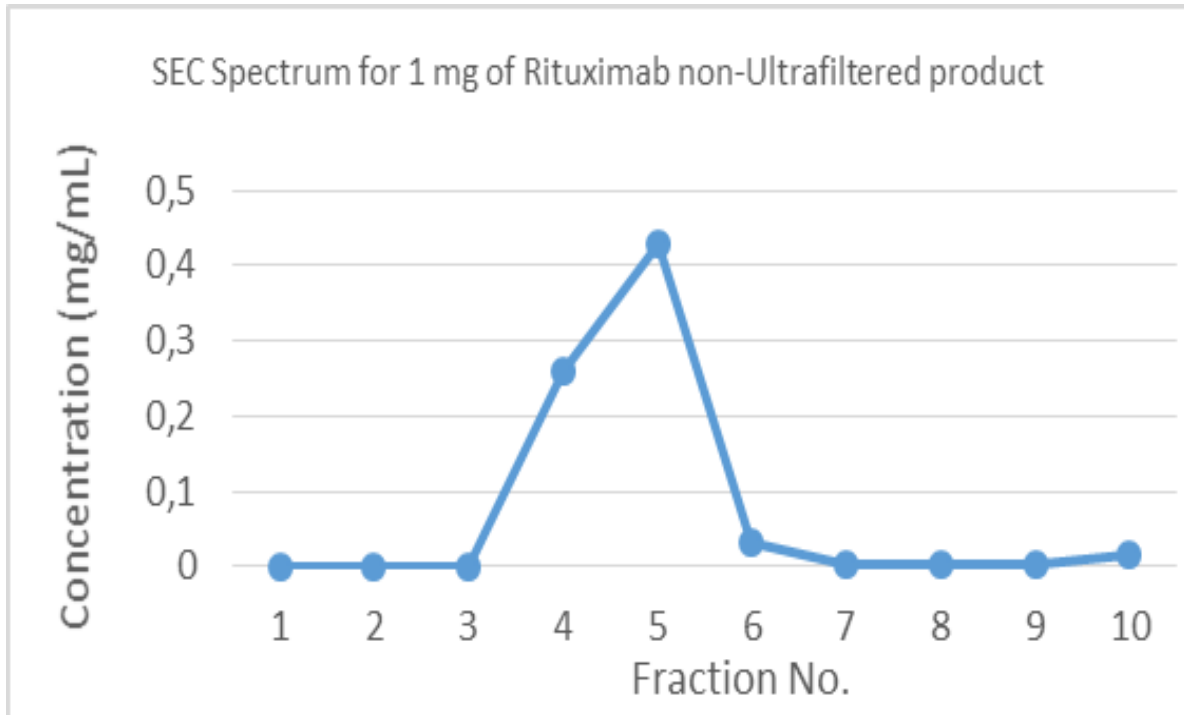
Figure 4. Comparison of the Size exclusion chromatography spectra for non-purified and purified rituximab solution.

Freeze drying of the antibody to determine a suitable protocol

The freeze drying protocol that we wanted to use was the key point of our investigation because many authors already used this method for preparing the kit containing rituximab (Park et al., 2012) (Gjorgieva Ackova et al., 2014). Gjorgieva Ackova et al. used the protocol of 3 days (highlighted in Fig. 5 below) as a suitable protocol for preparing the same kit (Gjorgieva Ackova et al., 2014).

In my work I wanted to compare their three-day protocol with a new two-day protocol that I expect would offer faster freeze drying, similar stability of the final product, similar quality and labeling yield.

As we can see from the figures 5 and 6, the differences in the two protocols are that the two-day protocol is devoid of the annealing step and the ramping times.

Table 3. 3-day freeze drying cycle

Segment	Freezing temperature	RAMP(Speed)	Holding Time
1 (Pre-freezing)	Room Temp to 4^0C	0.4^0C/min	30 minutes
2 (Freezing)	4^0C to -45^0C	0.4^0C/min	3 hours
	-45^0C to -15^0C	0.15^0C/min	6 hours
	-15^0C to -45^0C	0.2^0C/min	2 hours
3 (Primary Drying)	-45^0C to -10^0c	0.15^0C/minute	28 hours
4 (Secondary Drying)	-10^0C to 25^0c	0.15^0C/minute	14 hours

Table 4. 2-day freeze drying cycle

Segment	Freezing temperature	RAMP(Speed)	Holding Time
1 (Pre-freezing)	Room Temp to 4^0C	1.0^0C/min	30 minutes
2 (Freezing)	4^0C to -45^0C	1.0^0C/min	5 hours
3 (Primary Drying)	-45^0C to -10^0c	0.15^0C/minute	28 hours
4 (Secondary Drying)	-10^0C to 25^0c	0.2^0C/minute	14 hours

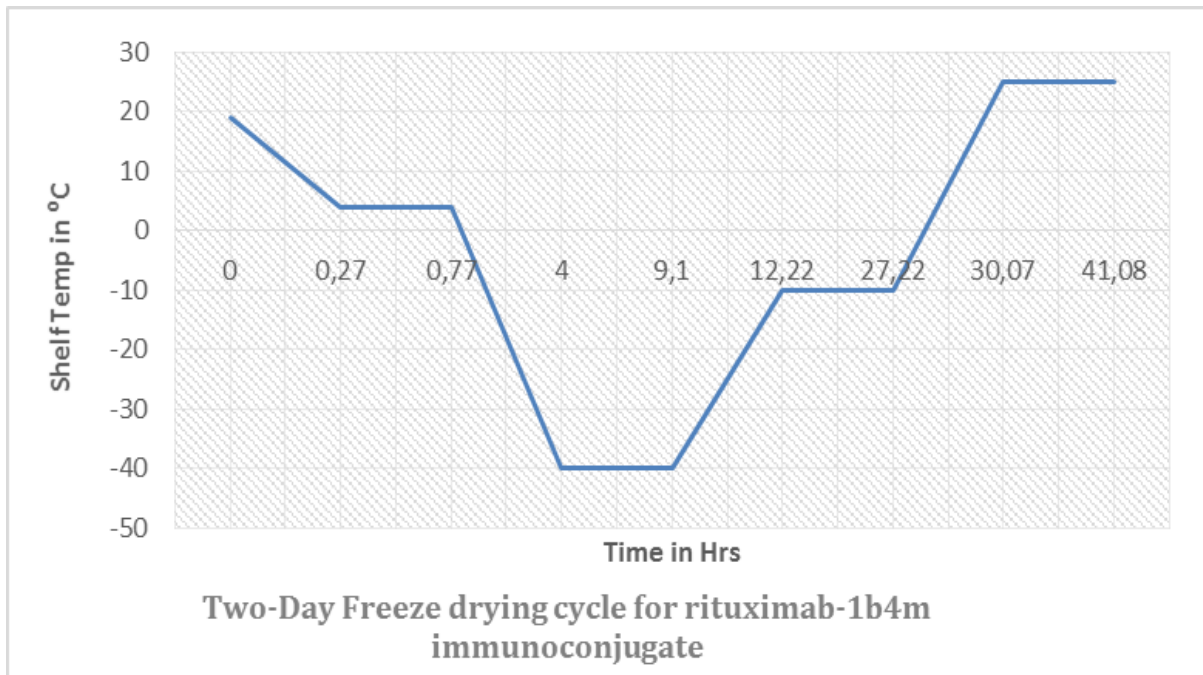Fig. 5. Graphic scheme of the three-day freeze drying protocol

Fig. 6. Graphic scheme for the two-day freeze drying protocol

After freeze drying we compared the size and appearance of the obtained "cake" of the final product. As we can see from the Figure 7 below, the cake is looking more consistent and contracted.
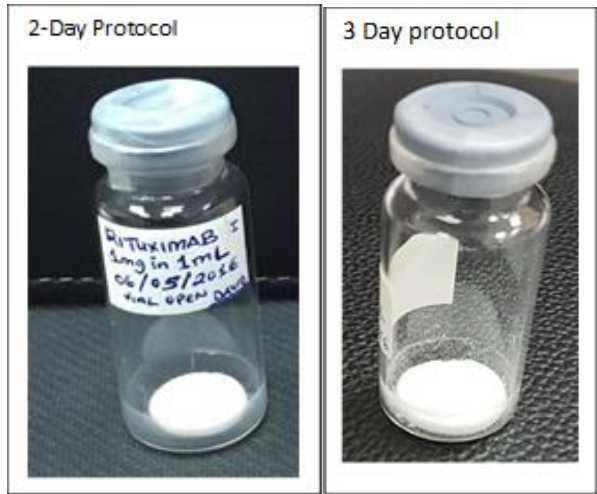
Fig. 7. Freeze dried rituximab cake products for the two-day and the three-day freeze drying protocols

Table 5: Average reconstitution times of freeze-dried rituximab products

Product	Reconstitution time (seconds)
3-day protocol	77.86
2-day protocol	68.38

As is visible from Figure 8 below, the solution of the products of three days and two days freeze drying protocols has similar clarity on visual inspection.
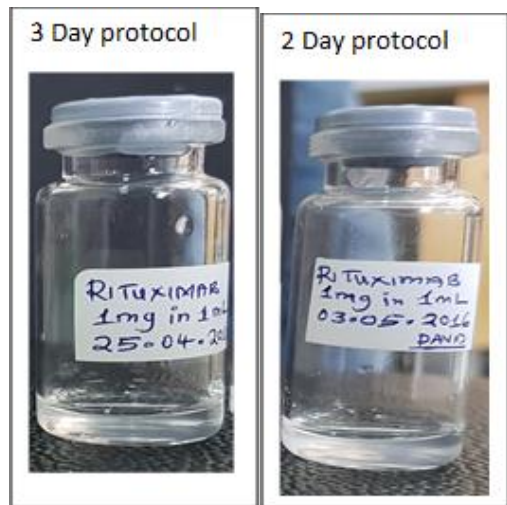

Fig. 8. Clarity of the reconstituted products of the two-day and the three-day freeze drying protocols

The reconstituted freeze dried immunoconjugates were tested using SEC to see if there was destruction of the complex after freeze drying. As seen from the SEC spectra in Figure 9 below, the peak of the product from the three-day protocol was broader (encompassing fraction numbers 4,5,6,7) than the peak obtained from the product of the two-day freeze drying protocol (contributed by fractions 4,5,6).
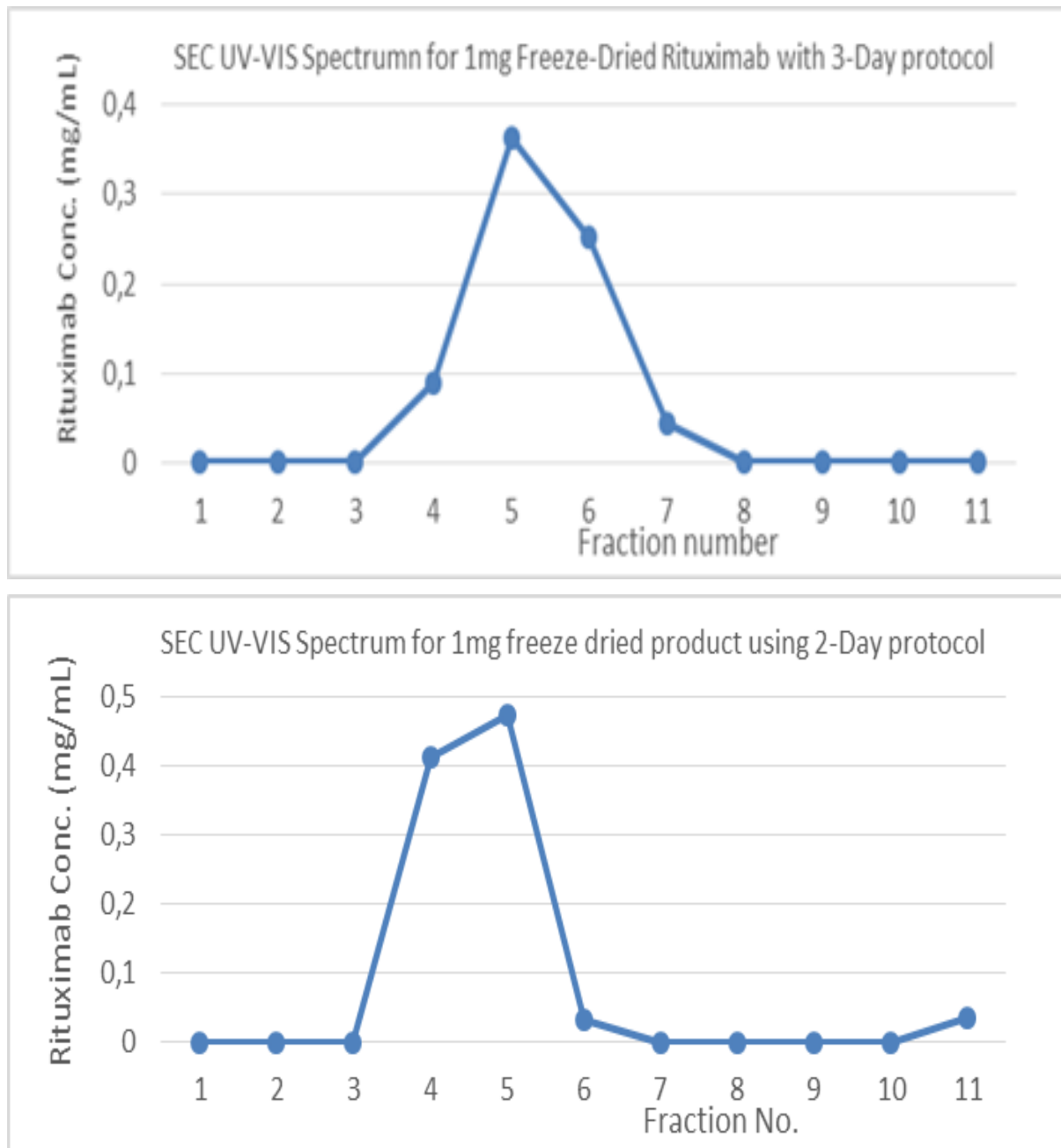

Fig. 9. Comparison the SEC spectra of rituximab from the three-day and the two-day freeze drying protocols
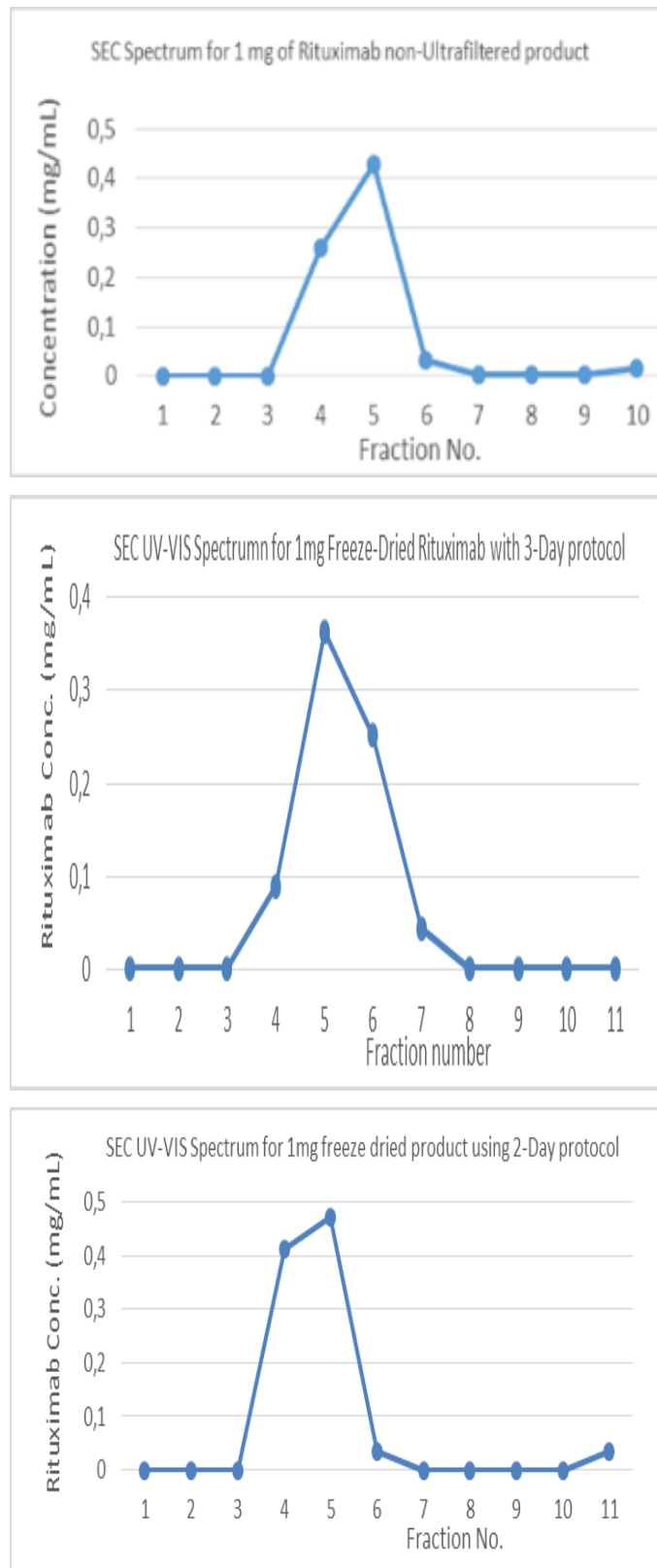
Fig. 10. Comparison between the SEC spectra of the rituximab in the commercial (MabThera®) product and the SEC spectra for freeze-dried rituximab products from different freeze drying protocols

Conjugation of rituximab with 1b4m-DTPA

The process of conjugation as described in the methods section above, was performed using the ligand 1b4mDTPA in 0.1M phosphate buffer pH 8.0 added to the purified antibody. The ratio of the antibody and ligand in the mixture of the complex rituximab-to-1b4mDTPA was 1:20. After the incubation period, the immunoconjugate mixture containing rituximab-1b4mDTPA was purified.

Purification of immunoconjugate

We used the same method of ultrafiltration for the purification of the immunoconjugate as we used for the antibody, as a more convenient method that does not necessarily damage the antibody.
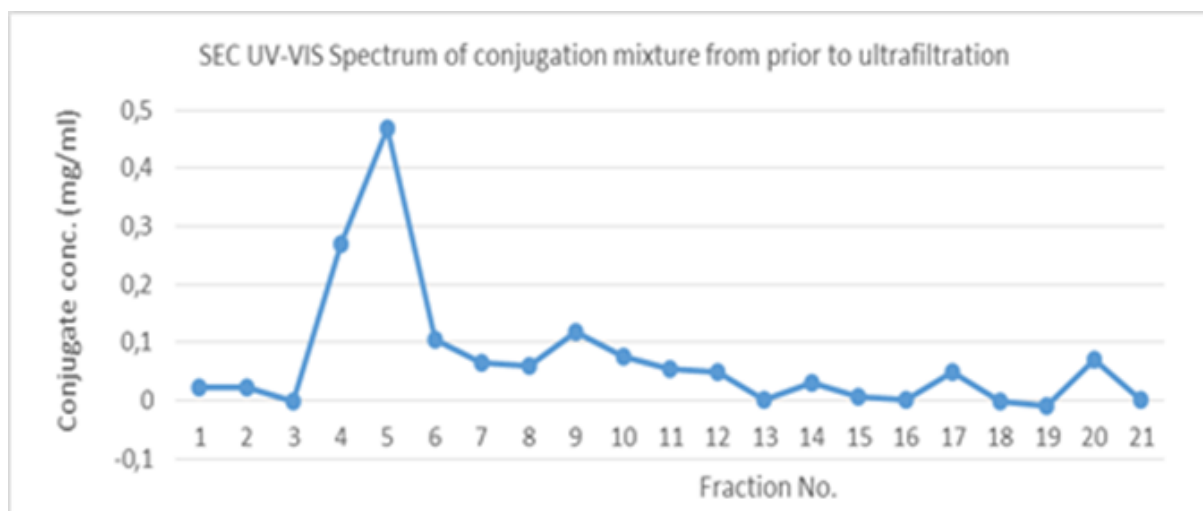

Fig. 11. SEC spectrum of a sample of the non-purified conjugation mixture

As we can see from Figure 11 above, the immunoconjugate rituximab-to-1b4mDTPA is the biggest of the multiple present peaks. After purification, as shown in Figure 12 below, the smaller peaks were eliminated, demonstrating the effectiveness of the purification process.
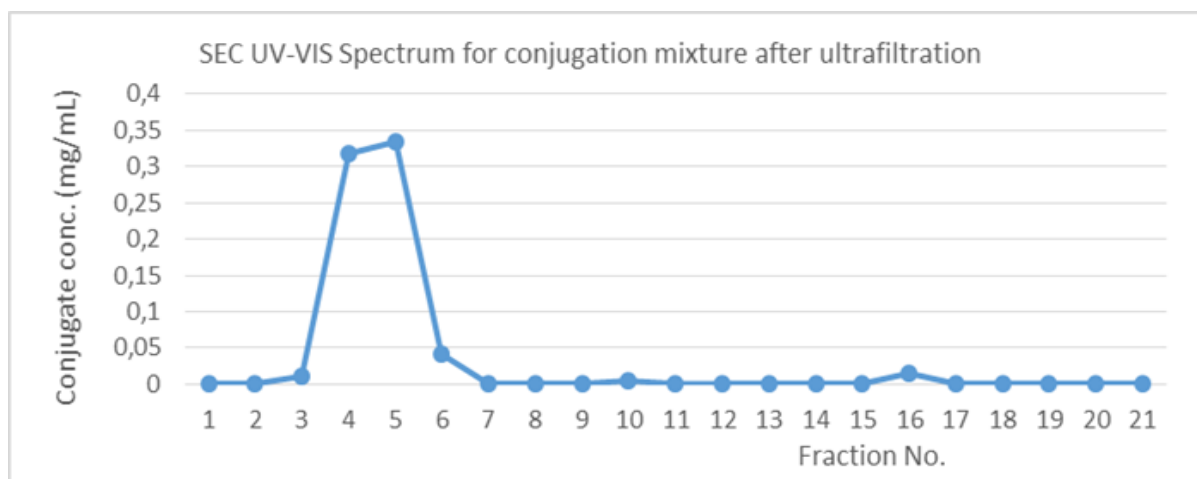
Fig. 12. SEC spectrum with UV-VIS detection for the purified immunoconjugate.

Concentration determination by UV-VIS spectrophotometry

After purification, we determined the concentration of the purified immunoconjugate as described in the methods section above. Then, the bulk immunoconjugate was reconstituted with 0.1M phosphate buffer pH 8.0 into a 13.7ml solution of 1mg/ml and stored at 2-8°C in a 15ml falcon conical centrifuge tube.

The purified immunoconjugate was used to prepare the freeze dried kit radio-pharmaceutical.

Freeze drying of the rituximab-1b4mDTPA immunoconjugate

For the freeze drying of the immunoconjugates we used the two days protocol that we had tested with rituximab. Its schema is depicted in Fig. 6 above. The cake is as shown in Figure 13. below.
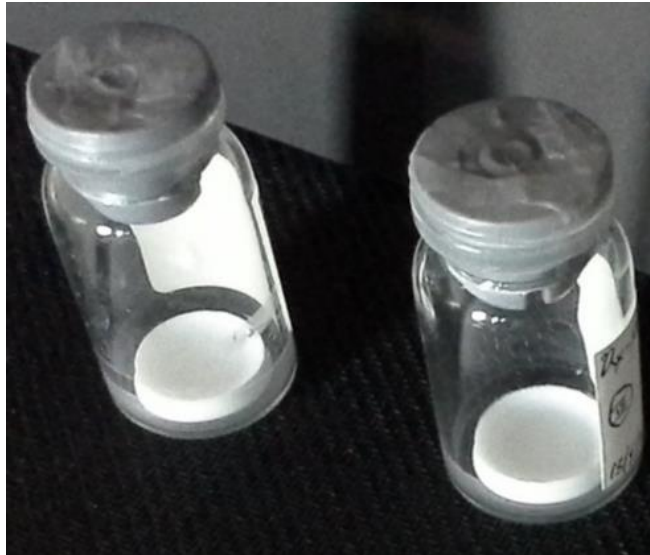
Fig. 13. Cake products of the freeze dried immunoconjugate

The freeze drying process normally reflects on the quality of the solution after the reconstruction of the freeze dried product. We did the reconstitution of the freeze dried product with 0.9% saline solution and the solution is as shown in Figure 14 below.

Reconstitution time for the rituximab-1b4m immunoconjugate was 30.88 seconds.

Fig. 14. Solution of reconstituted freeze dried immunoconjugate

'**Cold' labeling and purification of 'cold'-labeled product**

Cold labeling was performed using ^{175}Lu or ^{89}Y as described in the methods section above. The goal of cold labeling was to use the same moles of the Lu or Y as they are clinically used with their respective radioisotopes in their recommended maximum therapeutic activities.
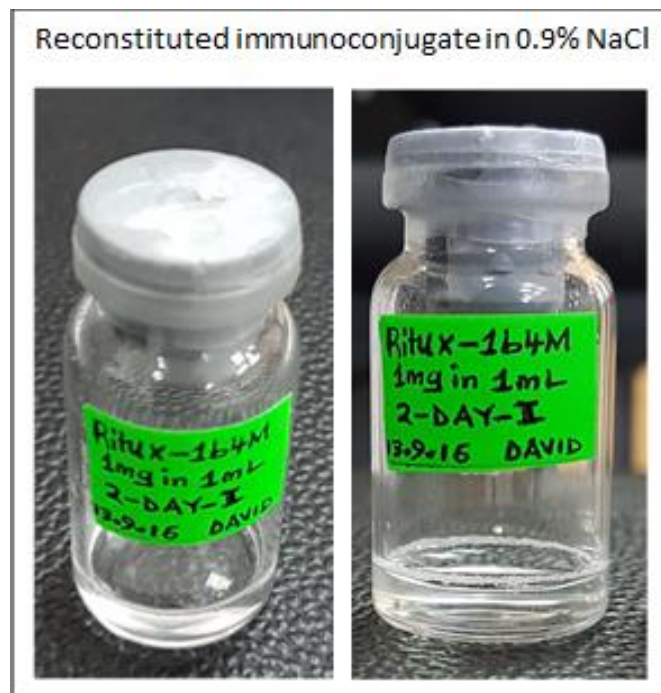
The calculated amount of ^{175}Lu used per 1mg of immunoconjugate was 1.061mcg and the amount of ^{89}Y used per 1mg of immunoconjugate was 0.0589mcg.

The chelation process is a stressful process to the immunoconjugate, in which case the immunoconjugate is expected to degrade to some extent. Sometimes, the chelation process is stressful enough to induce significant damage to the immunoconjugate.

It is, therefore, prudent to monitor this critical process. In our case, we investigated this by running SEC on a sample of the chelate for the purpose of informing us of the need for post labeling purification.

The expected outcome was demonstrated in the SEC spectrum as shown in Figures 15 and 16 below.

SEC for a sample of chelation mixture of Y-1b4mDTPA-rituximab
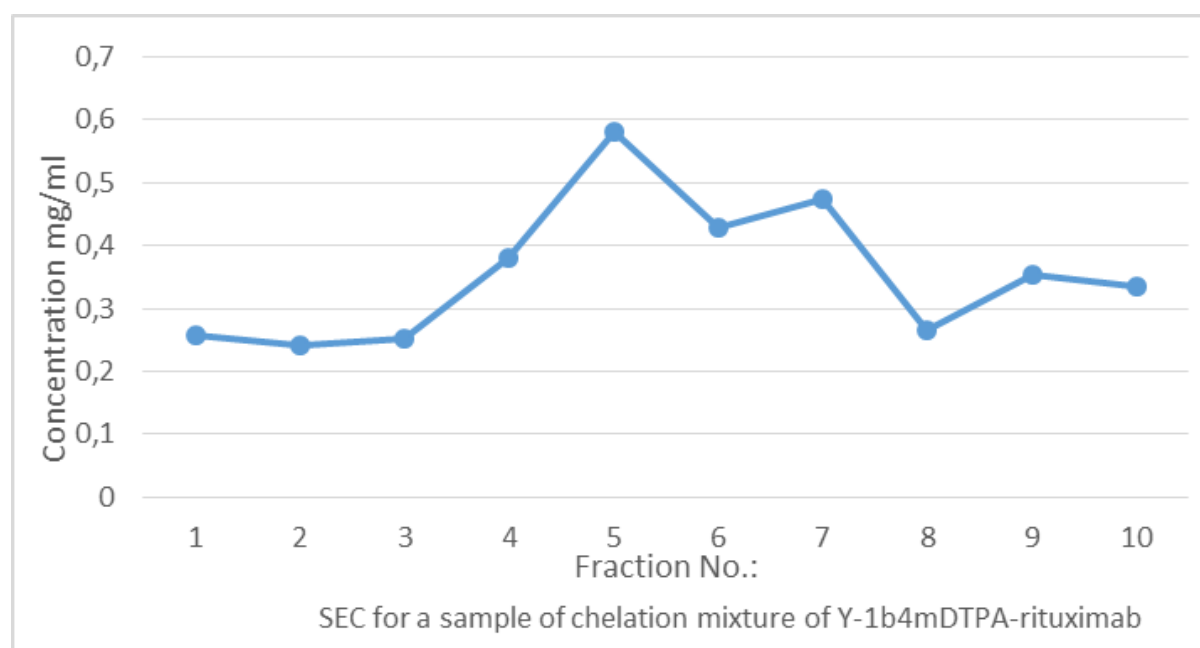
Fig. 15. Size exclusion chromatography for the chelation mixture of immunoconjugate with yttrium
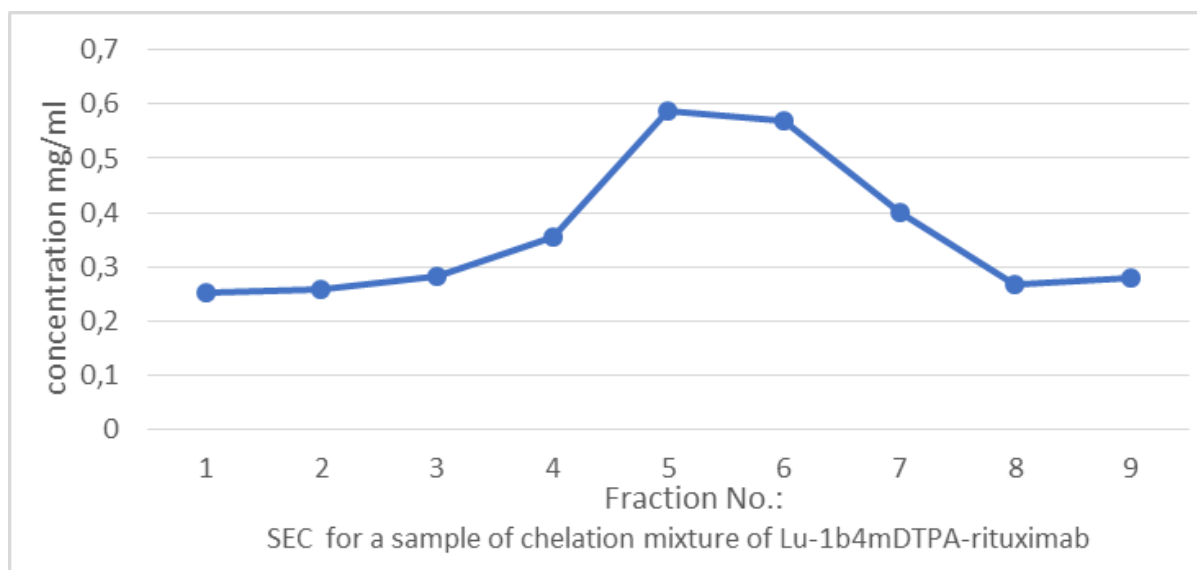
Fig. 16. Size exclusion chromatography for the chelation mixture with lutetium

Qualitative investigations by Fourier transform infrared (FTIR) spectroscopy

FTIR is a very useful technique for studying the molecular structural integrity of a protein in liquid formulations and also in solid formulations.

For our experiment, the FTIR spectra were obtained using the procedure described in the methods section above.

Using this technique, we studied:

- three days freeze dried rituximab,

- two days freeze dried rituximab,

- two days freeze dried rituximab-1b4m immunoconjugate,

- non-freeze dried rituximab commercial product,

- non-freeze dried rituximab-1b4mDTPA immunoconjugate,

- lutetium chelated non-freeze dried rituximab-1b4m-DTPA,

- yttrium chelated non-freeze dried rituximab-1b4m-DTPA,

- 0.9% saline solution of two days freeze dried rituximab-1b4mDTPA,

- ultra-filtered non-freeze dried rituximab-1b4m DTPA solution,

- lutetium chelated freeze dried rituximab-1b4mDTPA solution and

- yttrium chelated freeze dried rituximab-1b4mDTPA solution.

Solid samples
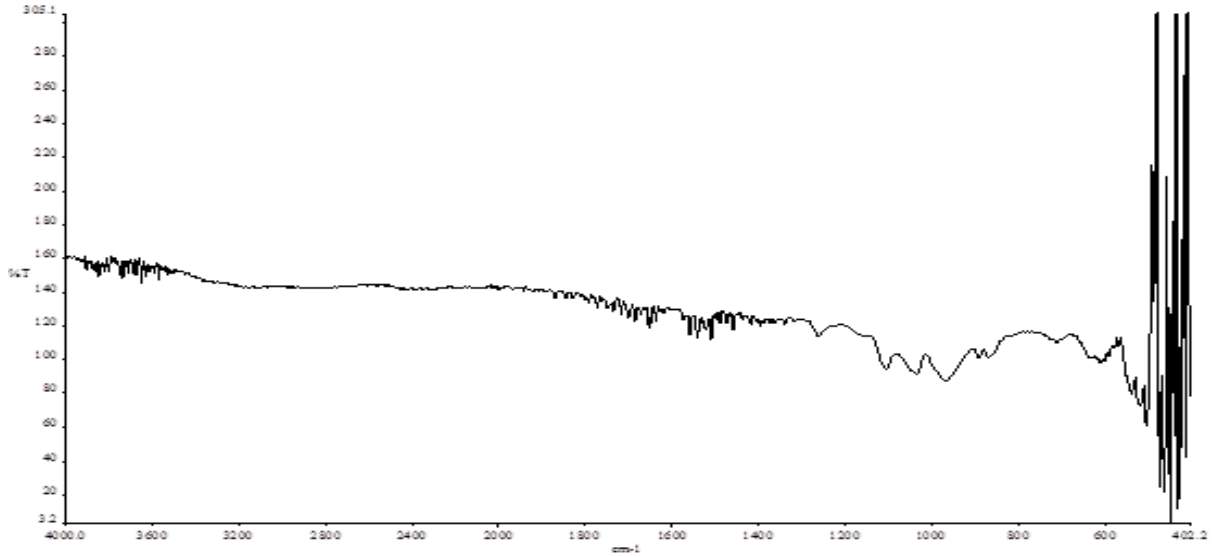
Fig. 17. ATR/FTIR spectrum for the three-day freeze dried rituximab product
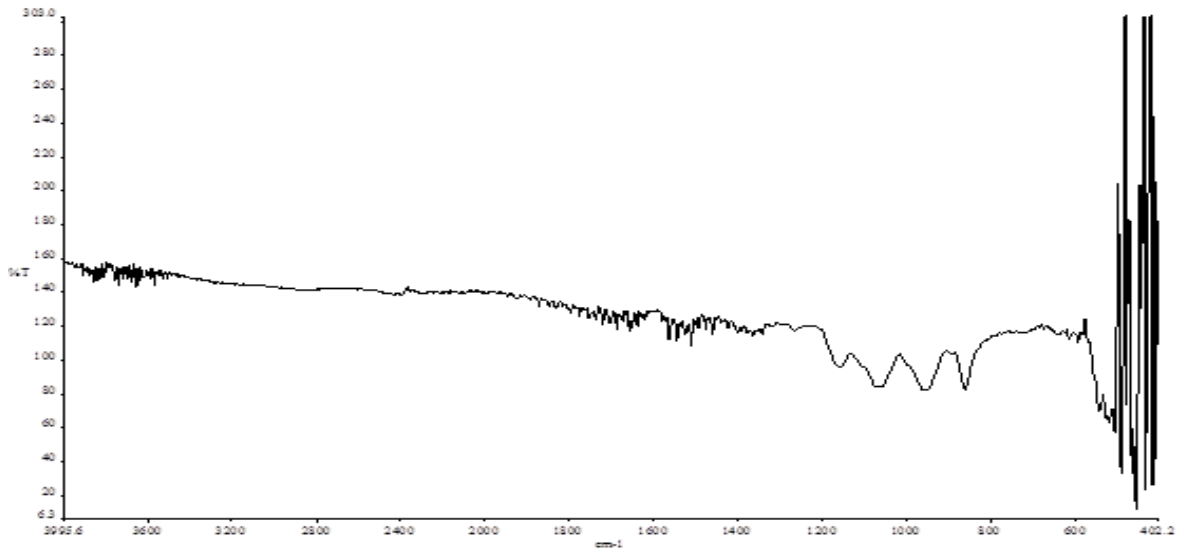
Fig. 18. ATR/FTIR spectrum for the two-day freeze dried rituximab product
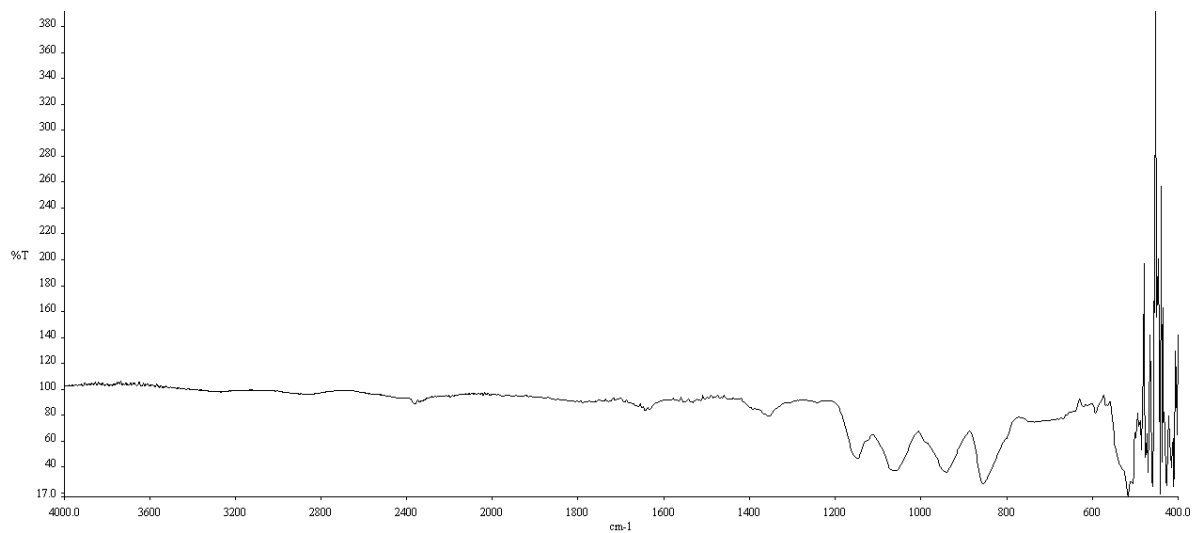
Fig. 19. ATR/FTIR spectrum for the powder two-day freeze dried rituximab-1b4mDTPA immunoconjugate

Liquid samples
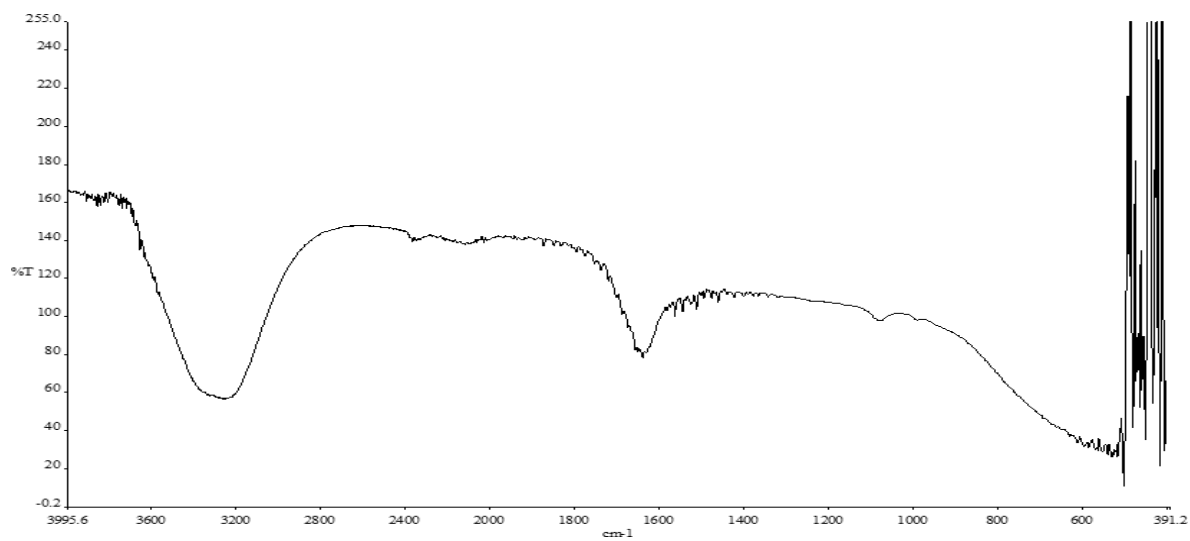
Fig. 20. ATR/FTIR spectrum for the non-freeze dried commercial rituximab liquid product
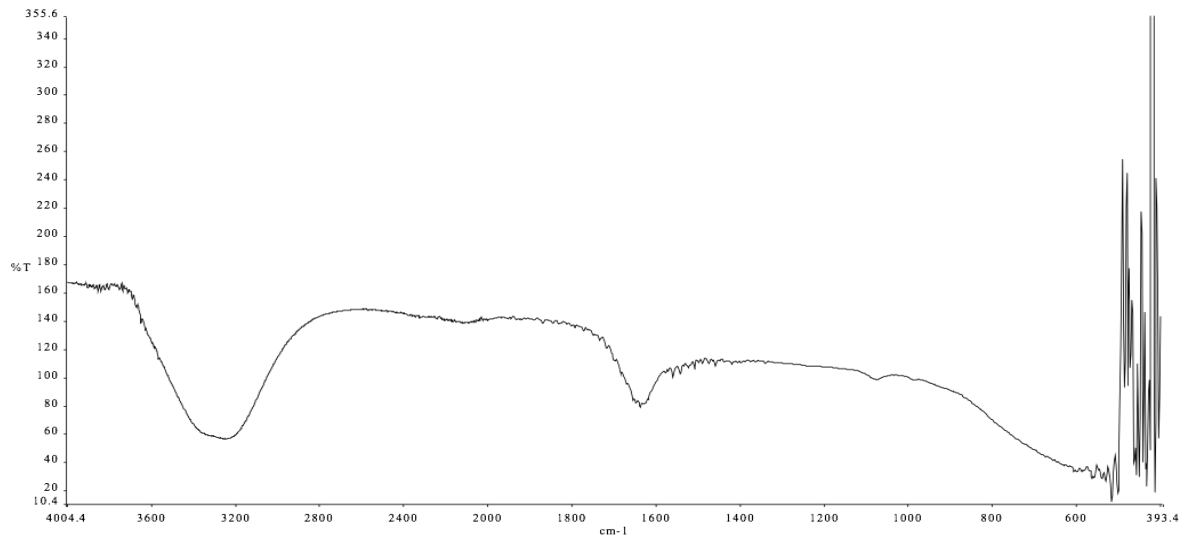
Fig. 21. ATR/FTIR spectrum of the solution of the non-freeze dried rituximab-1b4mDTPA immunoconjugate

Fig. 22. ATR/FTIR spectroscopy of the lutetium chelated non-freeze dried rituximab-1b4m-DTPA

Fig. 23. ATR/FTIR spectroscopy of the yttrium chelated non-freeze dried rituximabq-1b4m-DTPA

Fig. 24. ATR/FTIR spectrum for the solution of two-days freeze dried rituximab-1b4mDTPA

Fig. 25. ATR/FTIR spectrum for the ultra-filtered non-freeze dried rituximab-1b4mDTPA solution

Fig. 26. ATR/FTIR spectrum for the lutetium chelated freeze dried rituximab-1b4mDTPA solution

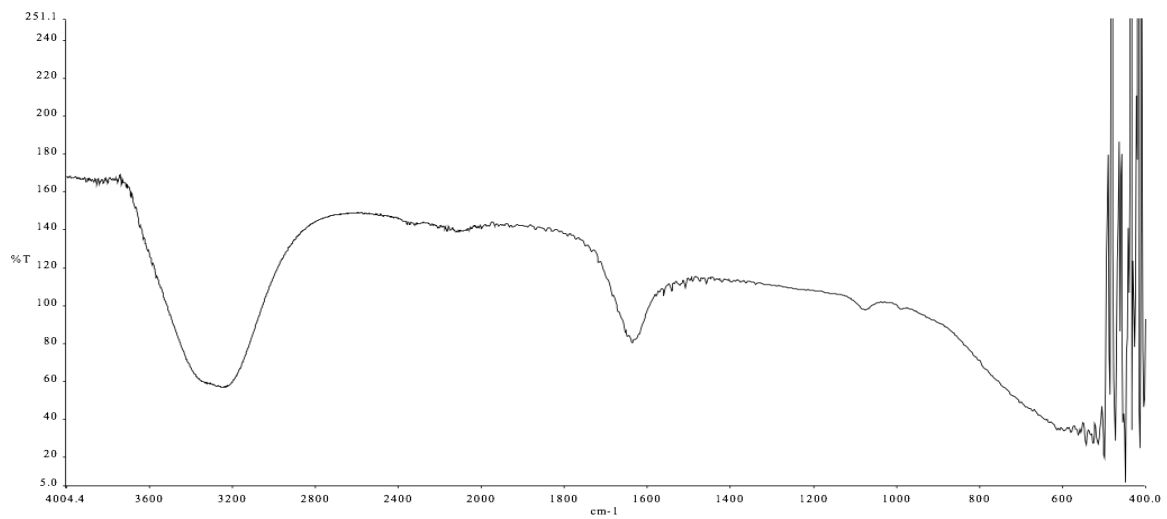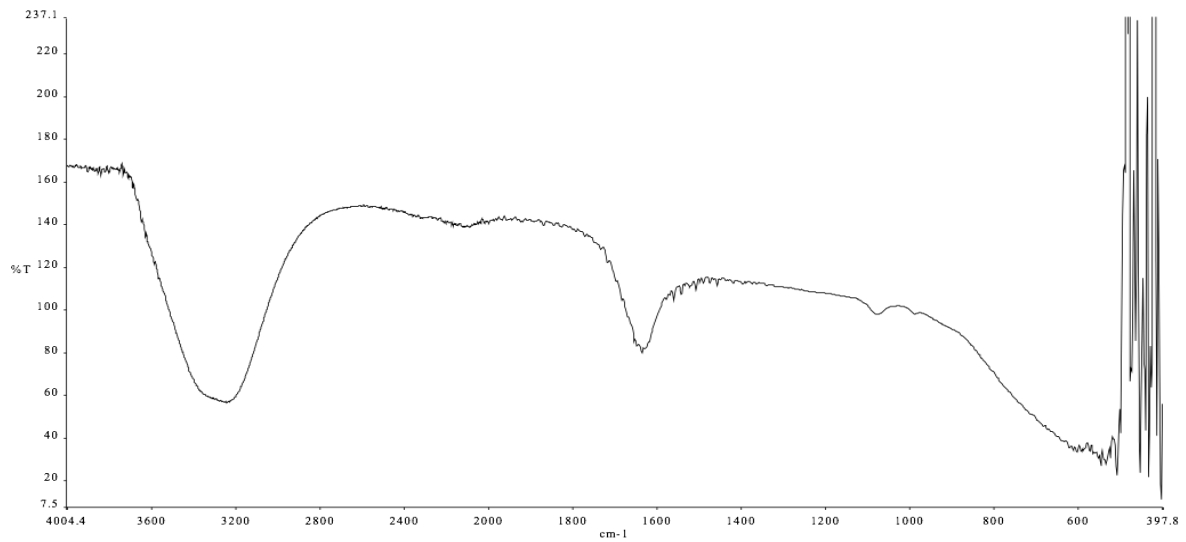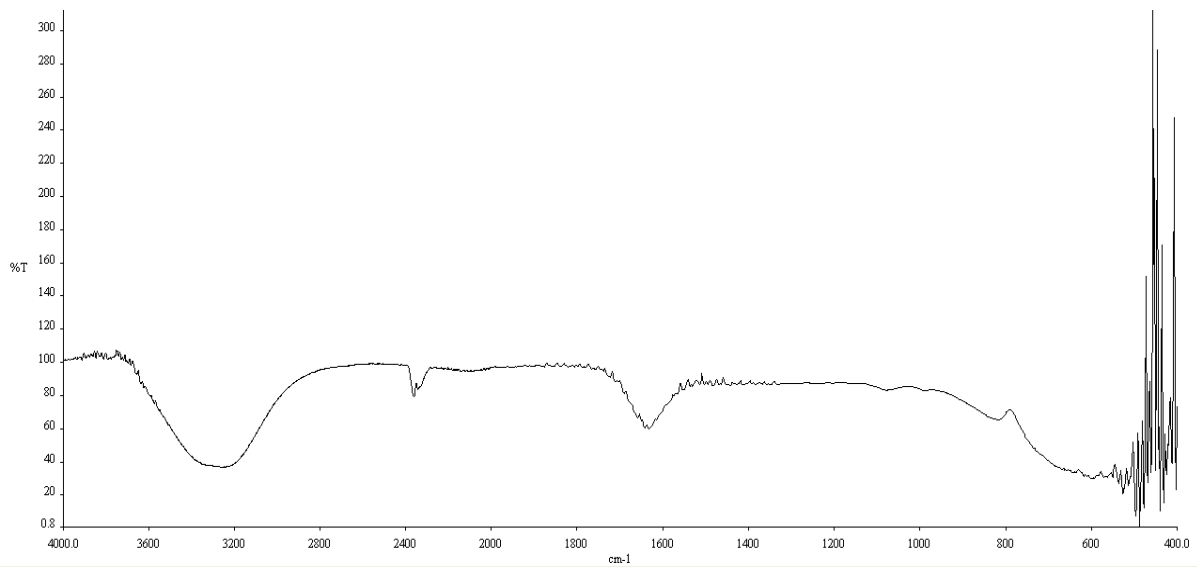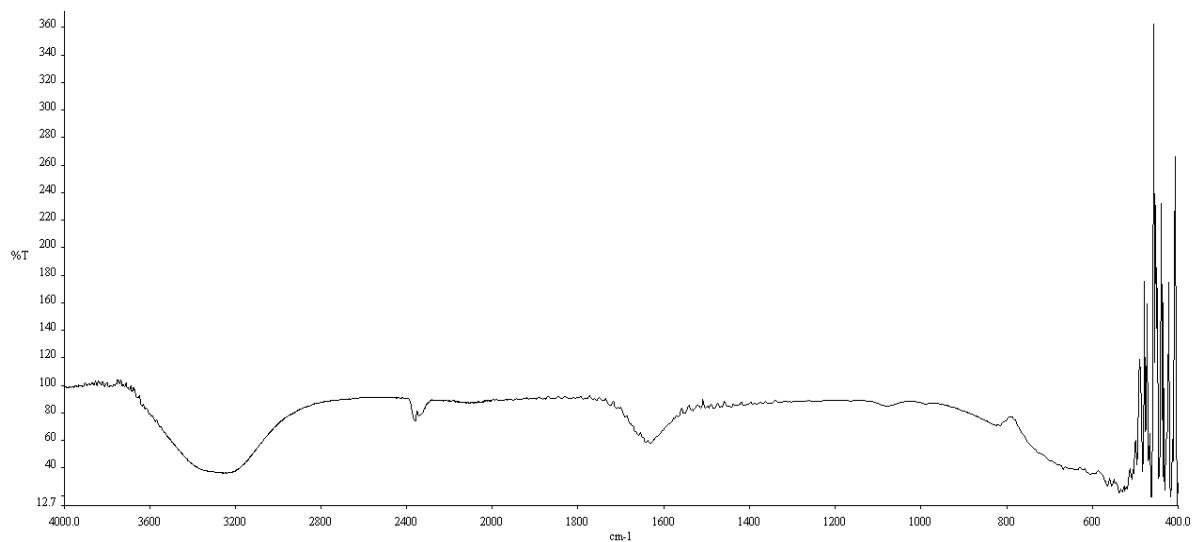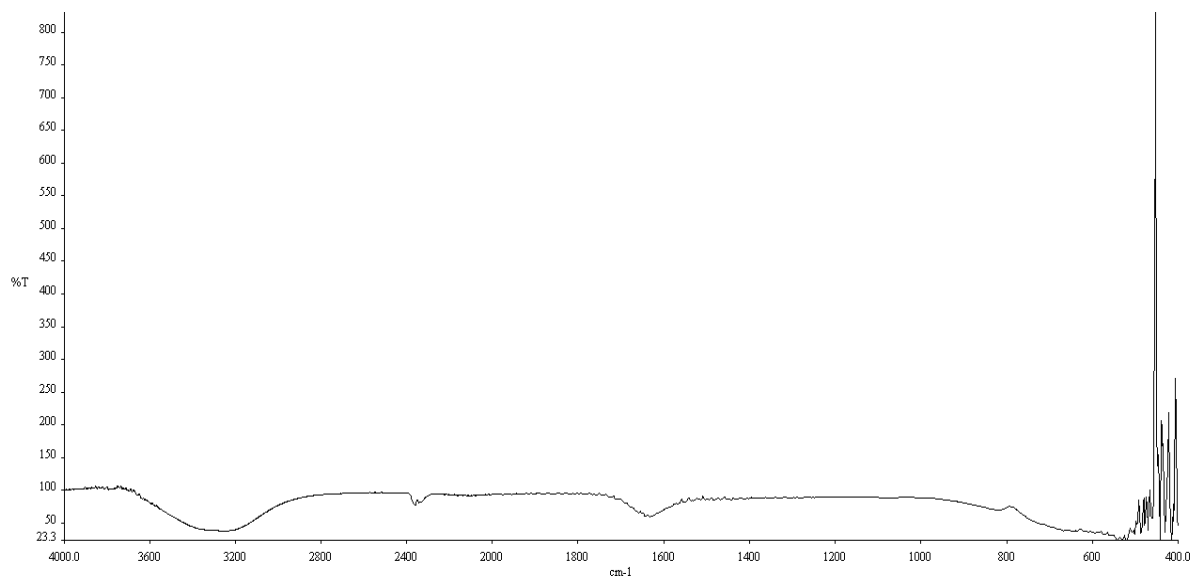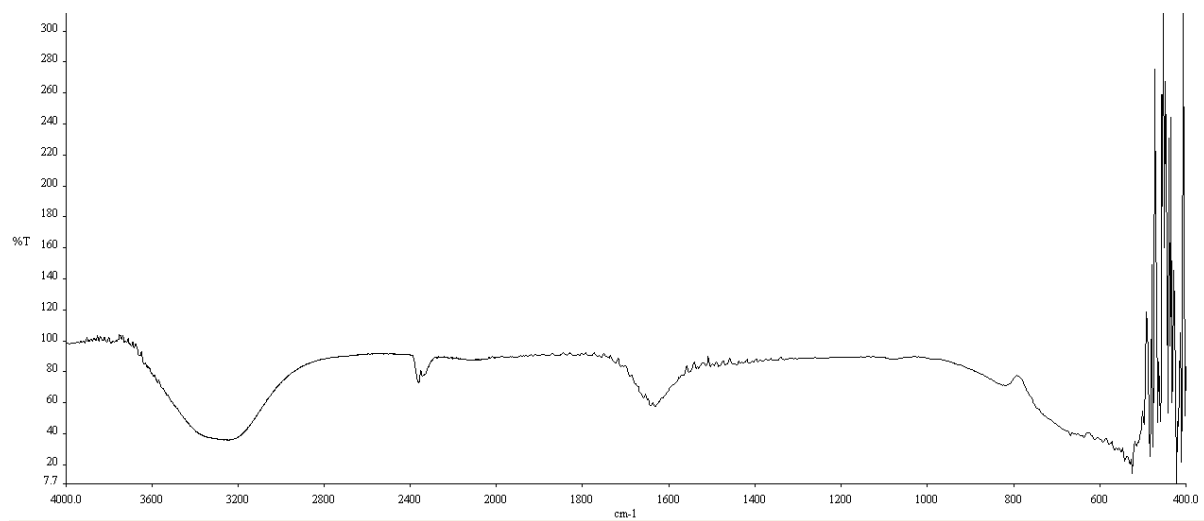Fig. 27. ATR/FTIR spectrum for the yttrium chelated freeze dried rituximab-1b4mDTPA solution

DISCUSSION

The use of TMAs for treatment of lymphomas is already widespread worldwide. There is a broad range of TMAs that are currently on the market or in research for use on NHLs. Among all those, rituximab continues to dominate the market significantly. Compared to the newer generation of TMAs for lymphoma treatment, rituximab is relatively less expensive and more accessible even in resource-poor countries. Also, rituximab is a chimeric TMA. In the area of radioimmunotherapy, all TMAs that have so far been registered for use on patients with lymphomas are murine and they expose treated patients to more adverse reactions and HAMA development. In addition, studies of this kind continue to attract huge interest from many researchers and the information base of radioimmunotherapy using rituximab immunoconjugates continues tremendously. These reasons and the fact that rituximab is already registered in most countries, already used as an adjunct with radioimmunotherapy of NHLs, and has an established efficacy and safety profile, led to the decision the decision to use rituximab for this study. With an optimized protocol, radiopharmacies would be capable of producing rituximab-1b4m radiopharmaceutical kits in their own countries using locally available rituximab commercial preparations.

The commercial rituximab product contains, apart from rituximab, excipients such as tween-80 and citrate buffer ("MabThera, INN-rituximab - WC500025821.pdf," n. d.). The rituximab had to be purified from these excipients so as to avert any potential interference with freeze drying, conjugation or chelation processes. Common antibody purification methods include dialysis, gel filtration, ultrafiltration, etc. (Liu et al., 2010). Ultrafiltration was used because it is easy to set up, inexpensive, fast, efficient and reliable. Using the 30kDa millipore ultrafilters, antibody light chains and other lower-than-30kDa molecules in the rituximab commercial product were sieved through the ultrafilters into the ultrafiltrate as the higher molecular weight rituximab whole TMA was retained. However, ultrafiltration has the possibility of increasing protein aggregation (Vázquez-Rey and Lang, 2011), structural changes and protein degradation due to the forces involved and also through antibody-antibody and/or antibody-membrane interactions. To minimize such potential adverse effects to the TMA, the least possible

number of ultrafiltration cycles were used. The necessary number of cycles were determined by performing a trial purification run of the rituximab commercial product with serial measurements of protein concentration in the ultra-filtrate by UV-VIS spectrophotometry at 280nm wavelength. The cycle number after which the ultrafiltrate protein concentration became undetectable was considered the least necessary and all other TMA purification runs were performed using the least necessary cycles. To recover the purified rituximab from the ultrafilter membranes, the ultrafilters were inverted and centrifuged. For the recovery, a one-hour centrifugation cycle was found to be adequate.

In the end, it was important to establish whether the purification was successful. This was achieved by comparing the protein purity of the impure commercial rituximab product and the purified product by their SEC spectra. The picture is as shown in Figure 20 below.
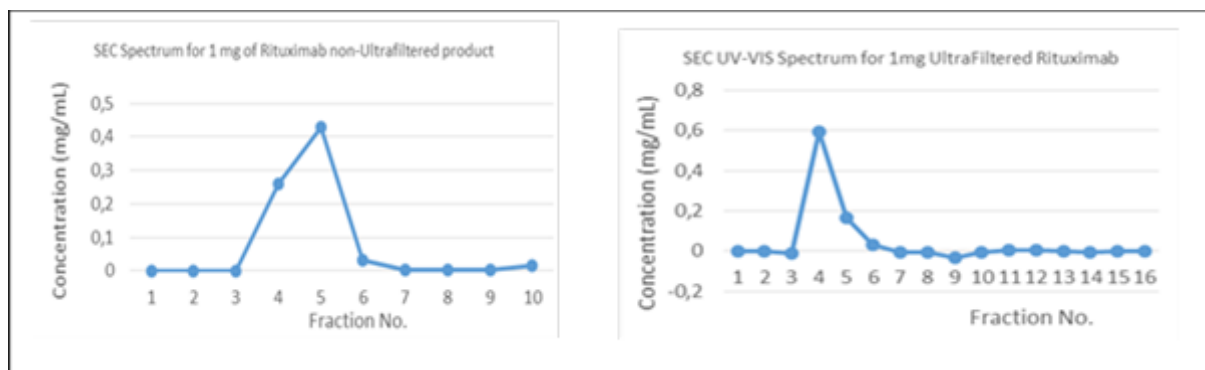
Fig. 28. Confirmation of effectiveness of purification of rituximab commercial formulation by comparison between SEC spectra of non-purified and purified samples

It can be seen that the small peaks attributed to 6th and 10th fractions were completely eliminated. Any minor impurities associated to such peaks were, therefore, successfully got rid of by ultrafiltration. Also, the 5th fraction was no longer the dominant peak following purification as it was decreased by 58% (from 0.43 mg/ml to 0.18mg/ml). In the impure sample, the desired whole TMA collected in the 4th fraction consisted of 35% of the expected 1mg protein in the sample. In contrast, the purified sample contained almost 60% of its protein content as the whole antibody (4th fraction). Peaks of 5th fraction may be attributable to antibody fragments larger than could

be filtered through the 30kDa millipore filter membranes, such as Fc and F (ab2)' fragments. Inasmuch as the 4th fraction is expected to carry some antibody aggregates formed from the antibody-antibody and antibody-membrane interactions during centrifugation at 5000 rpm, significant amounts could have been collected in 2nd, 3rd or even 1st fractions. Testing for antibody aggregates at 410 nm wavelength by UV-VIS spectrophotometry revealed that the 3rd fractions in both spectra contained the highest amounts of aggregates while they were undetectable in the 4th fractions. The observation was in agreement with the observations made by other authors (Katarina S. 2014). It is evident from Figure 20 above that the purification process was adequate considering the increase in the higher molecular weight peak height accompanied with a decrease in the lower molecular weight peak heights. After the successful purification, we deemed the antibody as ready for conjugation with the bifunctional chelating agent 1b4mDTPA.

The freeze drying protocol that we wanted to use was a two-day protocol and it was the key point of our investigation. Many authors have already used the three-day freeze drying method for studying kit formulations containing rituximab-1b4mDTPA (Gjorgieva Ackova et al., 2014). In this work we wanted to compare the three-day protocol with the new two-day protocol that can potentially provide faster time of freeze drying, higher stability of the final product, same quality and good radiolabeling yield with either yttrium-90 or lutetium-177.

In this study, the new freeze drying protocol was tested with the non-conjugated antibody with the expectation that the findings obtained therefrom would provide information on the suitability of the protocol for freeze drying of the immunoconjugate. The non-conjugated antibody was also freeze dried via the three-day protocol. The products emanating from the two freeze drying protocols were compared in terms of their cake appearance, SEC spectra and UV-VIS spectra. A comparison of the above parameters between the freeze dried products and the non-freeze dried rituximab solution was also made so as to determine the effect of each protocol on the rituximab. During freeze drying, the antibody molecule is expected to undergo some reversible unfolding in the dry product (Carpenter et al., 2002). A well freeze dried product ensures that the antibody folds back to its biologically active tertiary and quaternary structures upon its reconstitution into its solution of final usage. We used a comparison of the clarity, FTIR spectra and SEC spectra of the solutions of reconstituted freeze dried

products with the clarity, FTIR spectra and SEC spectra of the non-freeze dried products to determine if our protocol was superior, inferior or non-inferior to the previously used three-day protocol. As demonstrated in Figures 7, 8 (above), 29 and 31 (below), our two-day free drying protocol was comparable to the previously studied three-day protocol.
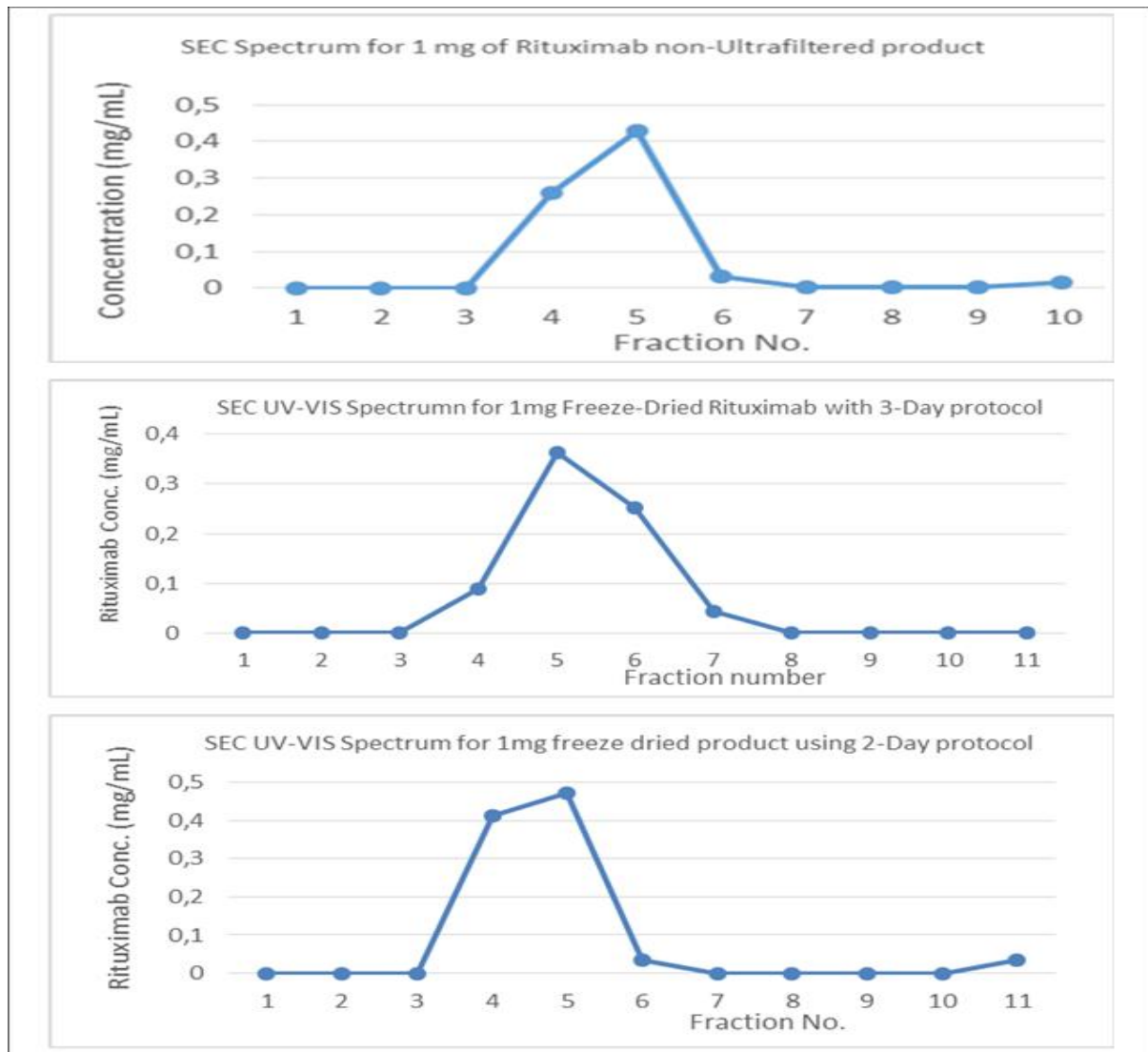
Figure 29. Comparison of the SEC spectra between the commercial rituximab product, 3-day freeze dried rituximab and 2-day freeze dried rituximab
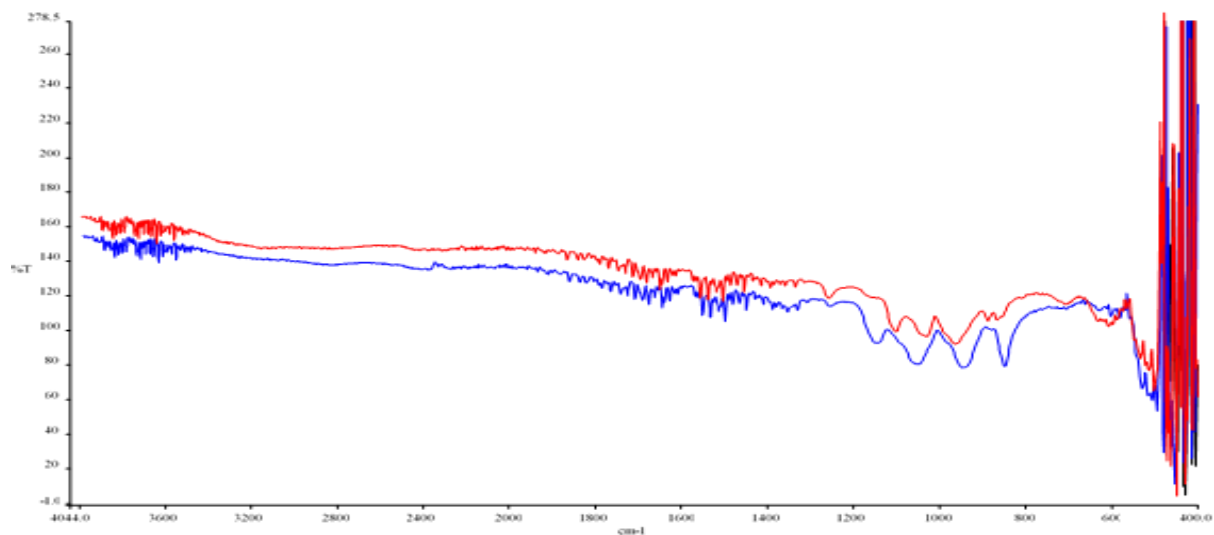
Figure 30. Comparison of the ATR/FTIR spectra of the powders from the 3-day freeze drying protocol (red) versus that of the 2-day freeze drying protocol (blue).
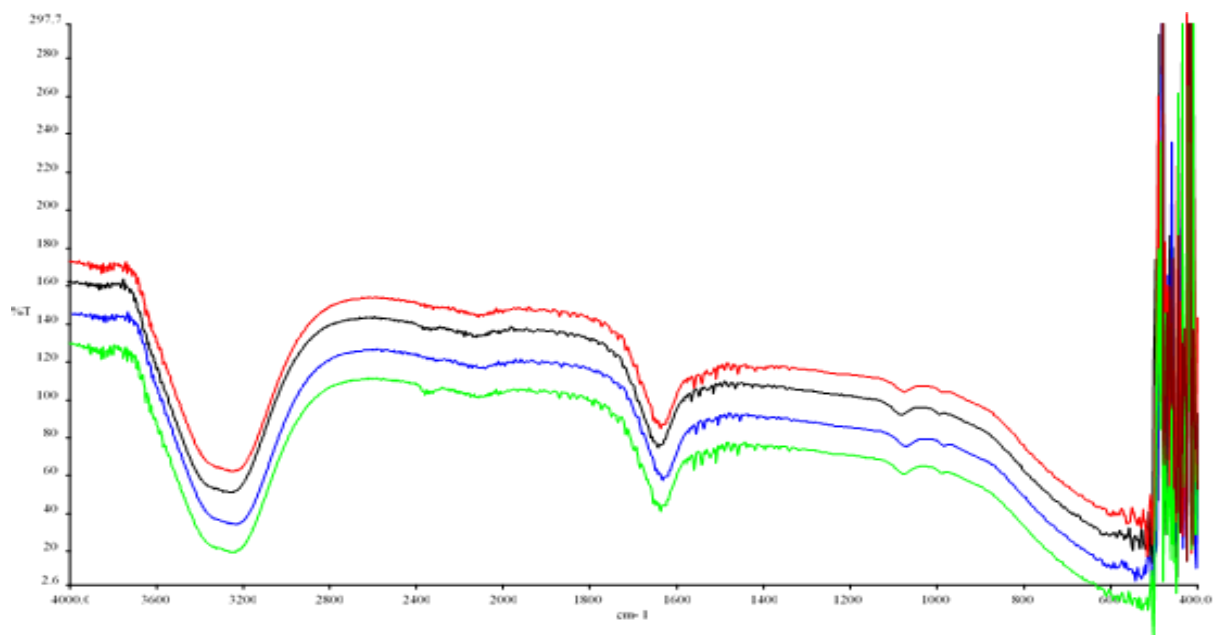
Figure 31. Comparison of the ATR/FTIR spectra of the reconstituted freeze dried rituximab powders (red – 2 day protocol, blue – 3 day protocol), commercial rituximab solution (green) and purified/ultra-filtered rituximab (black).

Conjugation of rituximab with an appropriate chelator for lutetium or yttrium was essential as rituximab hardly chelates these metals directly (Liu, 2008). Since this kit preparation is designed for post-labeling, conjugation of the antibody with the chelator into an immunoconjugate prior to radiolabeling was done.

The choice for the post-labeling approach is informed by the fact that the conjugation chemistry is more controllable and more suitable for kit formulation (Tolmachev et al., 2014). An already established conjugation protocol was used (Thakral et al., 2014). In previous studies (Gjorgieva Ackova et al., 2015), the conjugation protocol yielded. Immunoconjugates with an average of 6 chelator groups attached to each antibody molecule.

The desired number of chelator groups per antibody molecule is considered to be about 5 or 6 (Cooper et al., 2011) (Cooper et al., 2012). Less than 4 chelator groups per antibody is more likely to produce less than effective specific activity of the radiopharmaceutical, whereas the affinity of the radiopharmaceutical to the receptor site is less than optimal if the chelator groups per antibody molecule is above 8, due to steric hindrance from the bulky chelator groups.

The team that used a similar conjugation protocol to our protocol confirmed an average chelator number of 6 per antibody molecule by using MALDI-TOF mass spectrometry (Gjorgieva   Ackova et al., 2014).

The purification of the immunoconjugate is an important step to obtain the pure product for labeling and to eliminate excess of the ligand and damaged and fragmented antibody.

Because we used molar ratio of antibody-to-chelator of 1:20, the presence of excess chelator is expected.
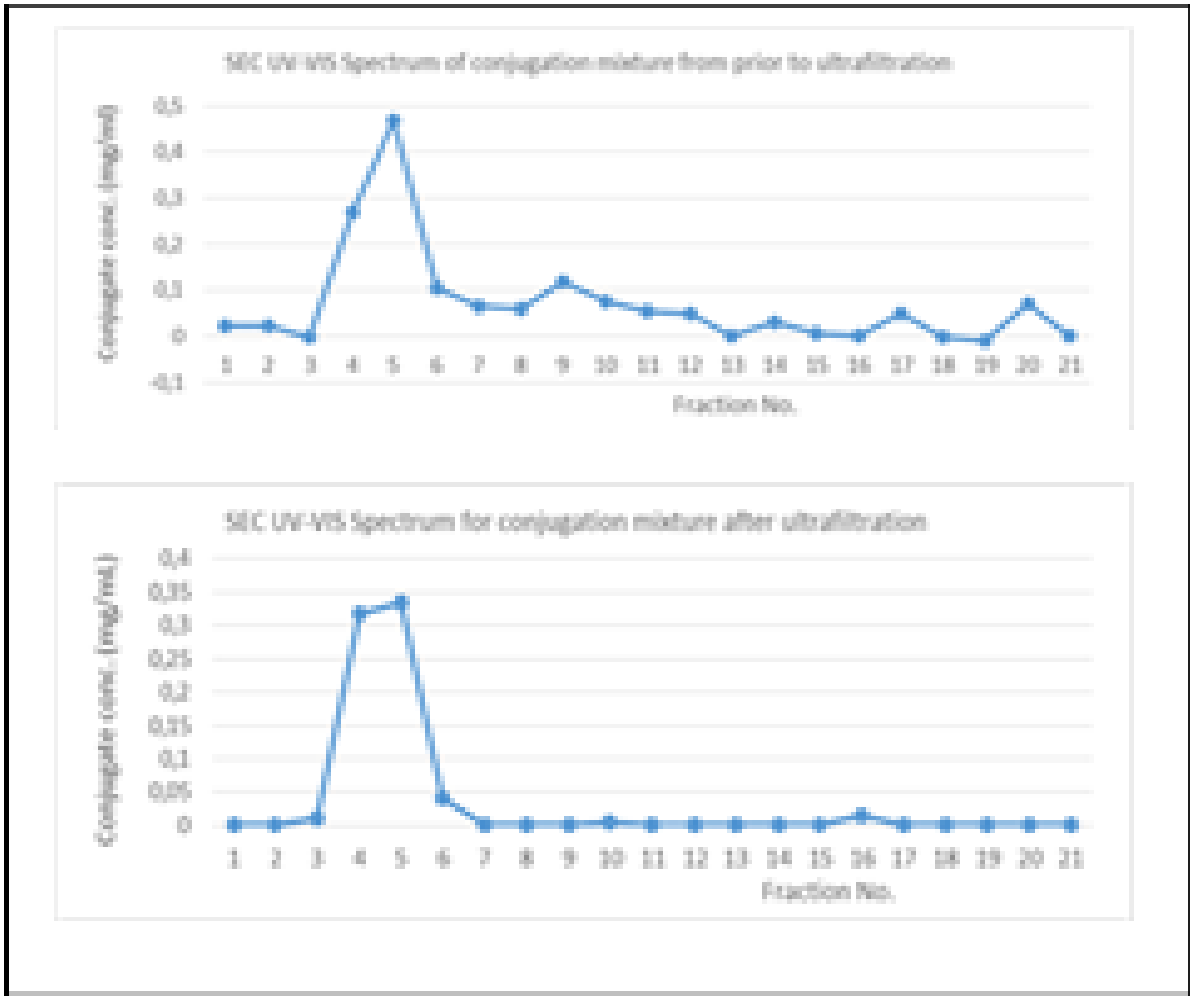
Figure 32. Comparison of the SEC spectra between the non-purified (above) and purified (below) immunoconjugate solutions

For the determination of the final concentration that we used for the kit formulation we needed to calculate the concentration of the immunoconjugate after purification. The minimum desired immunoconjugate concentration for the kit formulation was 1mg/ml.

After purification using ultra-filtration we determined the concentration measuring the samples of each fraction with UV-VIS spectrophotometry.

The final concentration was 6.85mg/ml in 2ml. This product was diluted accordingly to a 13.7ml 1mg/ml solution that corresponded to our need.

The selected protocol for freeze drying of the immunoconjugate was the two-days protocol as described in the methods section above.

The obtained results as presented in the results section confirm that this protocol is

also appropriate for the freeze drying of the immunoconjugate.

Fig. 33. Comparison by visual inspection of the appearance of the freeze dried cakes of rituximab by 3-day freeze drying protocol (left), rituximab by 2-day freeze drying protocol (middle) and immunoconjugate by 2-day freeze drying protocol (right).

The cold labeling was performed by chelation of the reconstituted immunoconjugate solution with $LuCl_3$ or YCl_3 using the protocol described in the methods section above. The goal of cold labeling is to use the same amounts of the Lu and Y as are used in their respective radioactive isotopes for the delivery of clinical therapeutic radio-activities (Kam et al., 2012) ("Zevalin_Package_Insert.pdf," n.d.).

Fig. 34. Comparison between the SEC spectra of the 'cold' labeled solutions of Y-immunoconjugate (left) and Lu-immunoconjugate (right).

As seen from the methods section above, we performed many manipulations on the antibody, starting from its approved comm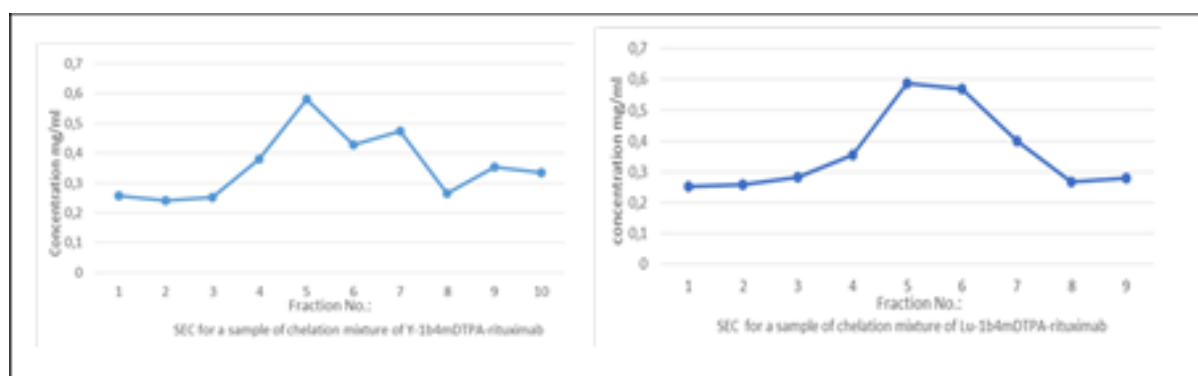ercial product up to the final metal chelated solutions. For that reason, we considered it of vital importance to investigate the molecular structures of all our products and more importantly, to compare the molecular structures of the processed products to the unprocessed products at each step. Since infrared spectroscopy is able to give us structural information (Barth, 2007), the FTIR spectra of the products were compared.

As seen from the results above, the two- day protocol yields an FTIR spectrum of the freeze dried powder that is similar to the spectrum obtained from the three-day pro-tocol that was previously studied. This finding demonstrates the possibility of achieving similar results as the three-day protocol with a shortened processing time.

Large proteins such as antibodies adopt complex structures when they are in their aqueous solutions. This results from the complex interactions that exist amongst the different amino acid residues and within the antibody molecules and between the amino acid residues and the surrounding water molecules. Freeze drying removes most of the free water in the environment of the antibody, leaving only the tightly bound water that is essential for avoiding plastic deformation of the protein molecules. From literature, it has been found that different freeze drying protocols may yield different protein molecular structures in the solid form as evidenced from FTIR spectra or Raman spectra. However, when the products of the different freeze drying protocols are reconstituted, the proteins relax back into their original secondary, tertiary and quaternary structures. In such cases, the FTIR spectra of the different liquid samples will be superimposable regardless of the spectra of their respective solid samples. When results of that kind are obtained, the different freeze drying protocols are adjudged to be suitable for the particular protein formulation. However, some freeze drying protocols may yield products that after reconstitution in aqueous solvents demonstrate FTIR spectra that are different from the spectrum of the parent product. Such freeze drying protocols are considered unacceptable on the account that they induce irreversible structural deformations on the antibody molecules and as such, they would be highly expected to impair the in vivo antigen binding of the antibody. In consideration of the foregoing, the structural integrity of the product after reconstitution and after metal chelation was of greater importance than that of the freeze dried solid immunoconjugate.

As shown from the results above, the FTIR spectra of the liquid samples of the commercial rituximab product, the purified rituximab, the freeze dried rituximab, the non-freeze dried immunoconjugate, the freeze dried immunoconjugate and the metal chelated products are superimposable. The observation that the FTIR spectra of all the products are superimposable provides an indication that the molecular structures of the products were not adversely affected by the manipulations. Such information is of paramount importance since the in vivo antigen binding of the radiolabeled antibody relies hugely on its structural integrity.

For the liquid FTIR spectra to be superimposable, not only the primary structures but also the secondary structures of the different antibody molecules need to be similar. Since this was achieved between the samples obtained with the three-day process of freeze drying in comparison with the products of the new two-day protocol, we were able to demonstrate that the shorter freeze drying protocol yields similar product characteristics to the already established three-day protocol.

CONCLUSION

The study confirmed that the purification method of ultrafiltration that had been used previously for similar studies was still suitable for purification of rituximab antibody form its excipients in MabThera without significant damage to the antibody. The purification method is therefore recommended for use in similar experiments.

Inasmuch as the conjugation protocol yielded the acceptable 4 – 8 chelator groups per antibody molecule, there was fragmentation of the antibody of up to 25% resulting into a yield of 75% for the conjugation step. Such antibody losses have a significant impact on the yield and cost of production of the immunoconjugate. Therefore, more studies for optimization of the conjugation protocol are recommended.

The freeze drying protocols of two days and three days yield products of similar quality. None of the freeze drying protocols produced detectable fragments. The cake appearance, reconstitution times and opacity on reconstitution were similar, demonstrating that the two freeze drying protocols yield products of similar quality.

In the radiolabeling conditions that were used, at least 30% fragmentation of the immunoconjugate occurred. The conditions for lutetium labeling caused less fragmentation of the immunoconjugate than the conditions for yttrium labeling. Therefore, optimization studies on the labeling protocol or introduction of a purification step post labeling are potentially beneficial.

From this study, we conclude that the two-day freeze drying protocol is non-inferior to the three-day protocol. It may, in fact, be superior to the three-day protocol based on the time and energy saved. More studies on the optimization and control of the critical freeze drying process parameters and the critical formulation attributes are also encouraged, as well as optimization of the conjugation and labeling protocols. Information continues to be sought that can support further development of the rituximab-1b4mDTPA kit radiopharmaceutical for NHL radioimmunotherapy.

REFERENCES

1. Abdelwahed, W., Degobert, G., Fessi, H., 2006. Freeze-drying of nanocapsules: Impact of annealing on the drying process. Int. J. Pharm., Selected papers from the 15th International Microencapsulation Symposium 324, 74–82.

2. Adams, H., Liebisch, P., Schmid, P., Dirnhofer, S., Tzankov, A., 2009. Diagnostic utility of the B-cell lineage markers CD20, CD79a, PAX5, and CD19 in paraffin-embedded tissues from lymphoid neoplasms. Appl. Immunohistochem. Mol. Morphol. AIMM 17, 96–101.

3. Approval Letter - Ibritumomab Tiuxetan, (Zevalin), IDEC Pharmaceuticals Corp- ucm113489.pdf [WWW Document], n.d. URL https://www.fda.gov/downloads/Drugs/DevelopmentApprovalProcess/HowDrugsareDevelopedandApproved/ApprovalApplications/TherapeuticBiologicApplications/ucm113489.pdf (accessed 3.3.17).

4. Barth, A., 2007. Infrared spectroscopy of proteins. Biochim. Biophys. Acta BBA - Bioenerg. 1767, 1073–1101.

5. Bhangoo, M.S., Karnani, D.R., Hein, P.N., Giap, H., Knowles, H., Issa, C., Steuterman, S., Pockros, P., Frenette, C., 2015. Radioembolization with Yttrium-90 microspheres for patients with unresectable hepatocellular carcinoma. J. Gastrointest. Oncol. 6, 469–478.

6. Boross, P., Leusen, J.H.W., 2012. Mechanisms of action of CD20 antibodies. Am. J. Cancer Res. 2, 676–690.

7. Brechbiel, M.W., 2008. Bifunctional Chelates for Metal Nuclides. Q. J. Nucl. Med. Mol. Imaging Off. Publ. Ital. Assoc. Nucl. Med. AIMN Int. Assoc. Radiopharmacol. IAR Sect. Soc. Of 52, 166–173.

8. Carpenter, J.F., Chang, B.S., Garzon-Rodriguez, W., Randolph, T.W., 2002. Rational Design of Stable Lyophilized Protein Formulations: Theory and Practice 109–133.

9. Chouvenc, P., Vessot, S., Andrieu, J., 2006. Experimental Study of the Impact of Annealing on Ice Structure and Mass Transfer Parameters during Freeze-Drying of a Pharmaceutical Formulation. PDA J. Pharm. Sci. Technol. 60, 95–103.

10. Cooper, M., Paul, R., Shaw, K., Blower, P., 2011. Which bifunctional chelator

for immunoPET with Cu-64? J. Nucl. Med. 52, 407–407.

11. Cooper, M.S., Ma, M.T., Sunassee, K., Shaw, K.P., Williams, J.D., Paul, R.L., Donnelly, P.S., Blower, P.J., 2012. Comparison of 64Cu-Complexing Bifunctional Chelators for Radioimmunoconjugation: Labeling Efficiency, Specific Activity, and in Vitro/in Vivo Stability. Bioconjug. Chem. 23, 1029–1039.

12. Davies, A.J., 2007. Radioimmunotherapy for B-cell lymphoma: Y90 ibritumomab tiuxetan and I131 tositumomab. Oncogene 26, 3614–3628.

13. Delgado, J., Matutes, E., Morilla, A.M., Morilla, R.M., Owusu-Ankomah, K.A., Rafiq-Mohammed, F., del Giudice, I., Catovsky, D., 2003. Diagnostic significance of CD20 and FMC7 expression in B-cell disorders. Am. J. Clin. Pathol. 120, 754–759.

14. DrugBank (Ed.), 2016. Rituximab. DrugBank.

15. Ecker, D.M., Jones, S.D., Levine, H.L., 2015. The therapeutic monoclonal antibody market. mAbs 7, 9–14.

16. Ekenlebie, E., Einfalt, T., Karytinos, A.I., Ingham, A., 2016. Pharmaceutical patent applications in freeze-drying. Pharm. Pat. Anal. 5, 407–416.

17. Else, M., Marín-Niebla, A., de la Cruz, F., Batty, P., Ríos, E., Dearden, C.E., Catovsky, D., Matutes, E., 2012. Rituximab, used alone or in combination, is superior to other treatment modalities in splenic marginal zone lymphoma. Br. J. Haematol. 159, 322–328.

18. Gjorgieva Ackova, D., Smilkov, K., Janevik-Ivanovska, E., 2014. Formulation and Characterization of "Ready to Use" 1B4M-DTPA-rituximab for Lu-177 Labeling. World J. Med. Sci. 11, 535–540.

19. Gjorgieva Ackova, D., Smilkov, K., Janevik-Ivanovska, E., Stafilov, T., Arsova-Sarafinovska, Z., Makreski, P., 2015. Evaluation of non-radioactive lutetium- and yttrium-labeled immunoconjugates of rituximab - a vibrational spectroscopy study. Maced. J. Chem. Chem. Eng. 34, 351–362.

20. Jacobs, S.A., 2007. 90 Yttrium ibritumomab tiuxetan in the treatment of non-Hodgkin's lymphoma: current status and future prospects. Biol. Targets Ther. 1, 215.

21. Janda, A., Bowen, A., Greenspan, N.S., Casadevall, A., 2016. Ig Constant Region Effects on Variable Region Structure and Function. Front. Microbiol. 7.

22. Johnston, K.M., Marra, C.A., Connors, J.M., Najafzadeh, M., Sehn, L., Peacock, S.J., 2010. Cost-Effectiveness of the Addition of Rituximab to CHOP

Chemotherapy in First-Line Treatment for Diffuse Large B-Cell Lymphoma in a Population-Based Observational Cohort in British Columbia, Canada. Value Health 13, 703–711.

23. Kam, B.L.R., Teunissen, J.J.M., Krenning, E.P., de Herder, W.W., Khan, S., van Vliet, E.I., Kwekkeboom, D.J., 2012. Lutetium-labelled peptides for therapy of   neuroendocrine tumours. Eur. J. Nucl. Med. Mol. Imaging 39, 103–112.

24. Kasi, P.M., Tawbi, H.A., Oddis, C.V., Kulkarni, H.S., 2012. Clinical review: Serious adverse events associated with the use of rituximab - a critical care perspective. Crit. Care 16, 231.

25. L. Parus, J., Pawlak, D., Mikolajczak, R., Duatti, A., 2015. Chemistry and bifunctional chelating agents for binding 177Lu. Curr. Radiopharm. 8, 86–94.

26. Lee, J., Cheng, Y., 2006. Critical freezing rate in freeze drying nanocrystal dispersions. J. Controlled Release 111, 185–192.

27. Liu, H.F., Ma, J., Winter, C., Bayer, R., 2010. Recovery and purification process   development for monoclonal antibody production. mAbs 2, 480–499.

28. Liu, S., 2008. Bifunctional coupling agents for radiolabeling of biomolecules and   target-specific delivery of metallic radionuclides. Adv. Drug Deliv. Rev., Delivery Systems for the Targeted Radiotherapy of Cancer 60, 1347–1370.

29. MabThera, INN-rituximab - WC500025821.pdf [WWW Document], n.d. URL http://www.ema.europa.eu/docs/en_GB/document_library/EPAR_-_Product_Information/human/000165/WC500025821.pdf (accessed 2.28.17).

30. Park, J., Nagapudi, K., Vergara, C., Ramachander, R., Laurence, J.S., Krishnan, S., 2012. Effect of pH and Excipients on Structure, Dynamics, and Long-Term Stability of a Model IgG1 Monoclonal Antibody upon Freeze-Drying. Pharm. Res. 30, 968–984.

31. Reichert, J.M., Valge-Archer, V.E., 2007. Development trends for monoclonal antibody cancer therapeutics. Nat. Rev. Drug Discov. 6, 349–356.

32. Rezvani, A.R., Maloney, D.G., 2011. Rituximab resistance. Best Pract. Res. Clin. Haematol. 24, 203–216.

33. Schneid, S.C., Gieseler, H., Kessler, W.J., Luthra, S.A., Pikal, M.J., 2011. Optimization of the Secondary Drying Step in Freeze Drying Using TDLAS Technology. AAPS PharmSciTech 12, 379–387.

34. Siegel, R.L., Miller, K.D., Jemal, A., 2017. Cancer statistics, 2017. CA. Cancer

J. Clin. 67, 7–30.

35. Srivastava, S.C., Mausner, L.F., 2013. Therapeutic Radionuclides: Production, Physical Characteristics, and Applications, in: Baum, R.P. (Ed.), Therapeutic Nuclear Medicine, Medical Radiology. Springer Berlin Heidelberg, pp. 11–50.

36. Strosberg, J., El-Haddad, G., Wolin, E., Hendifar, A., Yao, J., Chasen, B., Mittra, E., Kunz, P.L., Kulke, M.H., Jacene, H., Bushnell, D., O'Dorisio, T.M., Baum, R.P., Kulkarni, H.R., Caplin, M., Lebtahi, R., Hobday, T., Delpassand, E., Van Cutsem, E., Benson, A., Srirajaskanthan, R., Pavel, M., Mora, J., Berlin, J., Grande, E., Reed, N., Seregni, E., Öberg, K., Lopera Sierra, M., Santoro, P., Thevenet, T., Erion, J.L., Ruszniewski, P., Kwekkeboom, D., Krenning, E., 2017. Phase 3 Trial of 177Lu-Dotatate for Midgut Neuroendocrine Tumors. N. Engl. J. Med. 376, 125–135.

37. Sugiura, G., Kühn, H., Sauter, M., Haberkorn, U., Mier, W., 2014. Radiolabeling Strategies for Tumor-Targeting Proteinaceous Drugs. Molecules 19, 2135–2165.

38. Thakral, P., Singla, S., Yadav, M.P., Vashist, A., Sharma, A., Gupta, S.K., Bal, C.S., Snehlata, Malhotra, A., 2014. An approach for conjugation of 177 Lu-DOTA-SCN- Rituximab (BioSim) & its evaluation for radioimmunotherapy of relapsed & refractory B-cell non Hodgkins lymphoma patients. Indian J. Med. Res. 139, 544.

39. Therapeutic Biologic Applications (BLA) > Bexxar Approval Letter 6/27/03 [WWW Document], n.d. URL https://www.fda.gov/Drugs/DevelopmentApprovalProcess/HowDrugsareDevelopedandApproved/ApprovalApplications/TherapeuticBiologicApplications/ucm128134.htm (accessed 3.3.17).

40. Tolmachev, V., Orlova, A., Andersson, K., 2014. Methods for Radiolabelling of Monoclonal Antibodies, in: Steinitz, M. (Ed.), Human Monoclonal Antibodies, Methods in Molecular Biology. Humana Press, pp. 309–330.

41. Uchida, J., Lee, Y., Hasegawa, M., Liang, Y., Bradney, A., Oliver, J.A., Bowen, K., Steeber, D.A., Haas, K.M., Poe, J.C., Tedder, T.F., 2004. Mouse CD20 expression and function. Int. Immunol. 16, 119–129.

42. Ujjani, C., Cheson, B.D., 2013. The current status and future impact of targeted therapies in non-Hodgkin lymphoma. Expert Rev. Hematol. 6, 191–203.

43. Vázquez-Rey, M., Lang, D.A., 2011. Aggregates in monoclonal antibody manufacturing processes. Biotechnol. Bioeng. 108, 1494–1508.

44. Witzig, T.E., Gordon, L.I., Cabanillas, F., Czuczman, M.S., Emmanouilides, C., Joyce, R., Pohlman, B.L., Bartlett, N.L., Wiseman, G.A., Padre, N., Grillo-López, A.J., Multani, P., White, C.A., 2002. Randomized Controlled Trial of Yttrium-90–Labeled Ibritumomab Tiuxetan Radioimmunotherapy Versus Rituximab Immunotherapy for Patients With Relapsed or Refractory Low-Grade, Follicular, or Transformed B-Cell Non-Hodgkin's Lymphoma. J. Clin. Oncol. 20, 2453–2463.

45. Yeong, C.-H., Cheng, M., Ng, K.-H., 2014. Therapeutic radionuclides in nuclear medicine: current and future prospects. J. Zhejiang Univ. Sci. B 15, 845.

46. Zevalin_Package_Insert.pdf [WWW Document], n.d. URL http://www.zevalin.com/downloads/Zevalin_Package_Insert.pdf (accessed 2.28.17a).

47. Zevalin_Package_Insert.pdf [WWW Document], n.d. URL http://www.zevalin.com/downloads/Zevalin_Package_Insert.pdf (accessed 3.2.17b).